C.P. No. 1389

C.P. No. 1389

PROCUREMENT EXECUTIVE, MINISTRY OF DEFENCE

AERONAUTICAL RESEARCH COUNCIL

CURRENT PAPERS

Impedance Measurements On A Spinning Model Helicopter Rotor

by

R. Cansdale

D. R. Gaukroger

Structures Dept., R.A.E., Farnborough Hants

LONDON: HER MAJESTY'S STATIONERY OFFICE

1978

£2-50 NET

UDC 534.231.3 : 533.662.6 : 533.661

*CP No.1389
July 1976

IMPEDANCE MEASUREMENTS ON A SPINNING MODEL HELICOPTER ROTOR

by

R. Cansdale
D. R. Gaukroger

SUMMARY

The technique for measuring rotor impedances at the shaft of a model rotor has been further developed. The present technique is described in the Report, and values of impedance are presented for a four-blade rotor of semi-rigid design operating at zero lift, zero advance ratio, and a range of rotational speeds. The problems of interpreting and applying rotor impedances are discussed.

---

* Replaces RAE Technical Report 76086 - ARC 37251

CONTENTS

		Page
1	INTRODUCTION	3
2	EXPERIMENTAL REQUIREMENTS	3
3	RIG DESIGN	4
	3.1 General	4
	3.2 Suspension systems	5
	3.3 Instrumentation	5
	3.4 Calibration	6
4	METHOD OF TEST AND ANALYSIS	6
5	INTERPRETATION OF IMPEDANCES	8
6	RESULTS	10
7	APPLICATION OF TEST RESULTS	11
8	DISCUSSION OF FUTURE WORK	12
9	CONCLUSION	13
Appendix A	Rotor details	15
Appendix B	'Shaft-fixed' and 'shaft-free' natural frequencies of a simple system	16
References		18
Illustrations		Figures 1-28
Detachable abstract cards		

1 INTRODUCTION

Several years ago, a technique for measuring the shaft impedances of a model rotor was developed at RAE[1]. At that time, the main aim in developing the technique was to enable measurements of rotor dynamic behaviour to be obtained in a form that would allow detailed comparisons to be made of experiment and theory. Extensive tests with the initial rig, which was described in Ref.1, indicated several areas in which improvements were necessary. In addition, it was obviously desirable to increase the size of rotor model that could be tested. These factors led to the building of a new rig, tower mounted, and capable of handling models of approximately 1/5 or 1/4 scale of a medium size helicopter. The original analysis system was replaced by an on-line Fourier Analyser, and this, in turn, led to changes in the excitation system. Further thought was also given to ways in which measured rotor impedances could be used, other than to check theory by a comparison of measured and calculated values. The possibility of using measured impedances to make a stability assessment by 'matching' the impedances with those of an associated fuselage, appeared worthy of investigation. Work on these lines is still continuing, alongside an extended programme of impedance measurement for a range of rotor configurations.

The purpose of this Report is to describe the technique that is currently used to measure rotor impedances and to present a complete set of measurements for a model rotor. The model tested was essentially a 1/5 scale representation of a current semi-rigid rotor, and the test results relate to a range of rotational speeds of zero lift and zero advance ratio. The Report also includes consideration of impedance interpretation, and of methods of using measured impedances in stability assessments.

2 EXPERIMENTAL REQUIREMENTS

The basic requirements of a test rig were established in Ref.1, and will be given here in a condensed form. It is assumed that the instabilities which are most likely to be investigated with the use of impedances are 'ground resonance' and 'air resonance in the hover'. The shaft motions significant in these instabilities are (Fig.1): (i) fore and aft translation, (ii) pitch, (iii) lateral translation, and (iv) roll. In the hover, fore and aft translation and lateral translation are synonymous, as are pitch and roll. The rig requirements reduce, therefore, to the provision of separate oscillatory motions of the rotor in translational and rotational directions, with a capability of measuring, for each motion, the force or moment required to produce that motion, together with the forces and moments required to prevent motions in other directions.

Thus, a four-component balance is required at the rotor shaft, together with means of excitation and measurement of shaft motion. The impedances are simply the forces and moments per unit velocity of motion (Fig.2). If for example, at a frequency ω, a translation velocity $Ve^{i\omega t}$ is produced by a translational force $F_T e^{i(\omega t+\alpha)}$ at a phase angle α with the velocity, the translational impedance due to translation is $\frac{F_T}{V} e^{i\alpha}$. If, at the same time, the moment required to prevent rotor pitch is $M_p e^{i(\omega t+\beta)}$, the pitch impedance due to translation is $\frac{M_p}{V} e^{i\beta}$ and so on for the remaining forces and moments. Each impedance is a complex function of frequency, and it is necessary to measure the real and imaginary parts of the forces and moments relative to the shaft motion over the whole frequency range of interest. This constitutes a severe data-collection problem, for there may be nearly 5000 measurements required for each rotor condition. Obviously, an essential test requirement is some form of rapid testing and analysis.

The model requirements are all-important if the test technique is to have any useful application. Each of the overall rotor forces (Fig.3) includes components of centrifugal, inertia, aerodynamic and elastic forces, and it is desirable to scale the rotor so that these components in the model bear the same relationship to one another as in the full scale rotor. This requirement can only be met with a so-called Froude-scaled model, in which the ratio of model to full-scale tip speed is equal to the square root of the linear scale, and the model is therefore operating at an incorrect Mach number.

It is not possible to operate a model at correct Foude and Mach numbers simultaneously. If a model is scaled for correct Mach number the gravitational forces will be too small in relation to the other forces. Although this may, in some cases, be an acceptable penalty to pay for achieving correct aerodynamic behaviour in compressible flow, there was no reason to adopt Mach scaling in the present tests.

3 RIG DESIGN

3.1 General

The rig design is, in principle, the same as that described in Ref.1, but several changes have been made in the detailed construction. The rig is now mounted on a steel-framed tower with the rotor 2.85m above floor level (Fig.4); the rotor-to-ground clearance is approximately one rotor diameter for a 1/5 scale model of a rotor of 14m diameter. The tower was designed for high rigidity, and

the lowest natural frequency is 45Hz. This is well above the main frequencies of interest for ground and air resonance investigations on a typical model.

The rotor is driven by a 5.6kW electric motor through a variable speed eddy-current coupling. A fine adjustment of shaft speed is obtainable and speed stability under a steady torque is ±0.5%. The motor is at the base of the tower, and the drive to the rotor is taken by a splined shaft, with universal joints at each end, to accommodate shaft motions of the rig.

3.2 Suspension systems

The rig allows alternative motions of either rotation of the drive shaft (and hence of the rotor) about a rotor diameter, or translation of the shaft in the plane of the rotor.

Rotation of the drive shaft is achieved, as in the earlier rig, by using a non-parallel linkage system (Figs.5 and 6). It was shown in Ref.1 that this system can be designed to approximate closely a fixed axis of rotation. In the rig described here, two degrees of angular motion are accompanied by displacements of the rotor centre of only 0.1mm vertically and 0.01mm horizontally.

Translation of the drive shaft is achieved by using linear ball bearings to support the rig. The bearings run on two horizontal steel bars allowing the rig to move along the bars (Figs.5 and 7). This system replaces the parallel motion linkage of the earlier rig[1] which had an unacceptably high level of motion in directions other than translation.

An electromagnetic exciter mounted near the top of the tower (Fig.7) applies a force to the main body of the rig to produce motion of the drive shaft. The exciter is driven by a current amplifier which is fed with a sinusoidal voltage from a sweep frequency generator (Fig.8).

3.3 Instrumentation

The forces and moments acting on the rotor shaft are measured by strain gauge bridges bonded to a thin-walled steel plinth which is an integral part of the shaft bearing housing and baseplate. A cut-away photograph is shown in Fig.9, and a diagram of the arrangement in Fig.10. It may be seen from Fig.10 that forces and moments applied to the rotor shaft are transmitted either through the bearing housing and thence through the strain-gauged section, or down the drive shaft. To avoid the latter, a torque coupling is inserted in the drive shaft and this transmits axial torque only. Thus all the forces and moments relevant to rotor impedance measurement are transmitted through, and measured at,

the strain-gauged section. The moments about axes in the plane of the rotor are obtained by adding appropriate proportions of the shear forces at the measurement section to the bending moments at that section. This is done immediately following the gauge-signal amplification, so that the gauge signals that are analysed are proportional to the forces and moments at and about the rotor.

Shaft motion is measured by a velocity transducer attached to the main body of the rig. The velocity is measured relative to the adjacent tower structure to which the transducer is attached.

The rotational speed of the rotor is measured from a lamp and photocell unit. The light source is interrupted one hundred times per shaft revolution by a perforated disc on the shaft, the photocell output being read by an electronic counter. A second photocell unit provides a once-per-revolution pulse which is used for triggering the input to the analyser at constant azimuth position of the rotor.

3.4 Calibration

It is desirable to calibrate the force and moment measurement system under conditions that are, as nearly as possible, the conditions of a rotor test. If a uniform rigid disc is fitted in place of the rotor the rig may be operated in spinning conditions and with shaft motions imposed. This procedure was followed, and, by making additional tests with the disc fitted above the rotor datum, the fore-and-aft force, pitching moment and rolling moment systems were calibrated in terms of the forces and moments generated by the disc in fore-and-aft translation and pitch motions. (Rolling moments arise from gyroscopic forces when the disc is pitching.) Lateral forces cannot be generated in this way and the lateral force system was calibrated by rotating an out-of-balance mass with the rotor shaft fixed. As a check on the calibration, static forces and moments were applied to the rotor shaft, with the shaft fixed and non-rotating.

4 METHOD OF TEST AND ANALYSIS

Early measurements on the rig, and on the rig of Ref.1, were made by discrete frequency testing. The force and moment signal analysis was an analogue process using a resolved components indicator to determine the real and imaginary components of each force signal relative to the rig velocity signal. The process was very slow, and, because of the large number of signals to be analysed, was extremely time-consuming. Moreover the rotor was subjected to

long periods of oscillatory loading, which led to concern about the possibility of fatigue failures. There were also analysis difficulties when the excitation frequency coincided with the rotational frequency of the rotor or with its multiples. These problems were overcome by using sweep-frequency testing and by replacing the analysis system by a Fourier analyser. These changes reduced the test time by nearly two orders of magnitude.

The method of test is to sweep the frequency from 1 to 35Hz in approximately 8 seconds. A chosen force or moment signal and the rig velocity signal are taken through identical low-pass filters and thence to the analyser where they are digitised and stored. The signals are sampled from the start of the frequency sweep for a period of 10 seconds. The impedance is obtained by dividing the Fourier transform of the time history of the force or moment signal by that of the velocity signal. The analyser can be programmed to carry out this process and to present the impedance in numerical and graphical form as the variation of the real and imaginary components with frequency. The analyser settings required to obtain impedance values every 0.01Hz result in an upper frequency limit of 50Hz for inputs to the analyser. The low-pass filters mentioned above are to attenuate higher frequencies and prevent aliasing.

In practice, the procedure described above is elaborated to eliminate the effects of forces generated in the rotor as a result of rotor asymmetries, and to correct for the impedances of the moving parts of the rig. The procedure is shown in Fig.11. Forces generated in the rotor are eliminated by taking records of forces and motions when no excitation is applied; these records are then subtracted from the records obtained with applied excitation. The impedances of the moving parts of the rig are obtained from tests without a rotor; the values are stored in the Fourier analyser and are subtracted from the measured rotor-plus-rig impedances at the final stage of analysis. A further elaboration is to repeat the measurement sequence a number of times, generally five, and to average the results.

When a rotor is under test, there is the possibility of an instability of the entire rig and rotor system occurring. Qualitatively, the rig may be regarded as a fuselage attached to the rotor, and if the 'fuselage' has certain characteristics a ground-resonance type of instability may occur. Even without instability, it is possible for the whole system to be so lightly damped that when the frequency sweep is applied the rig response reaches the limits of travel at certain frequencies. To avoid this situation, with its attendant risks

of rig and rotor damage, a position servo system was installed to limit excess motion. A displacement transducer mounted at the top of the tower provides a signal proportional to the displacement of the rotor shaft from some datum position. This signal is amplified and used to drive the electromagnetic exciter to produce a force opposing the displacement. The frequency sweep signal is fed into the servo amplifier. The response of the servo system does vary somewhat with frequency, but, since the motion of the rig is being measured, this is not important.

5 INTERPRETATION OF IMPEDANCES

Before discussing impedance interpretation, it is as well to be clear about the rotor conditions in which the classical impedance concept, and the technique of 'impedance-matching' are valid. An impedance, in the classical sense, exists if an excitation at a particular frequency results in a response at the same frequency and only at that frequency. For a rotor which is excited in a fixed direction (Fig.12) the response will satisfy this classical impedance definition only in the hovering condition, and provided the rotor has three or more blades. In forward flight, (or with a two-blade rotor in hovering flight) an excitation at a particular frequency will give rise to responses both at the original frequency and also at other frequencies which are dependent on the rotational speed. The measurement of rotor impedances is only valid, therefore, in the hover, and this restricts its application to the investigation of hover phenomena such as ground-resonance, hovering air-resonance and the forced response of the aircraft in the hover.

In fact, because the latter seldom gives rise to problems, impedances are of only limited use for determining forced responses. For this reason only stability applications are discussed in this Report.

In considering the interpretation of impedances, it is first assumed that a complete set of impedance measurements has been made on a rotor at a rotor speed and collective pitch appropriate to a full scale condition. Eight impedances are measured as functions of frequency, and symmetry allows a (4×4) impedance matrix to be obtained (Fig.13). This measured data may be used in various ways. If the measurements have been made in order to determine the stability behaviour of the rotor when it is mounted on a specific fuselage, then it is necessary to derive, either by measurement or calculation, a (4×4) impedance matrix of the fuselage for shaft motions corresponding to those of the rotor measurements. For a rigid fuselage in the hover, for example, the impedance terms will be simple frequency

functions of the mass and moments of inertia of the fuselage (Fig.14). The procedure is to add the rotor and fuselage impedance matrices term by term (and, within each term, frequency by frequency). The resulting matrix (Fig.15) contains all the data required to calculate the dynamic behaviour of the combined rotor fuselage system. If the elements of the matrix had been derived as analytical expressions, the complex roots of the system could be obtained by equating the determinant of the matrix to zero. However, with the matrix in numerical form, probably the easiest approach is to calculate the response of some point in the system to a sinusoidal force at each frequency for which data have been measured. The resulting response vector can then be analysed by standard numerical or graphical methods to obtain the mode frequencies and damping ratios. This approach has the advantages that it presents the results in a form familiar to the dynamicist, it gives a physical feel for the behaviour of the system, and it indicates an instability by revealing any modes that have negative damping. (These will be characterised on the vector plot by modal arcs which rotate anti-clockwise with increase of frequency.) The disadvantage of the method is that it implicitly involves inverting the impedance matrix, and this is likely to emphasise experimental errors which, even with the most stringent efforts to obtain measurement accuracy, may well be significant at the modal frequencies of the system.

To appreciate why this should be so, it is instructive to examine a simple, if impractical, rotor-fuselage system. A hovering helicopter is postulated in which the only motional freedom of the rotor shaft is in a fore-and-aft direction and the only blade mode is a lag mode. To assess the stability of the machine it is only necessary to measure a single impedance - the fore-and-aft force per unit fore-and-aft velocity. The impedance may have the form of Fig.16. There are two peaks resulting from excitation of the blade lag mode at frequencies corresponding, to the shaft-fixed lag mode frequency plus and minus the rotational speed. It is important to note that the impedance peaks occur at frequencies dependent on the shaft-fixed lag mode frequency. If, however, the impedance is inverted, so that the velocity response per unit input force is obtained, the two peaks are then related to the shaft-free lag mode frequency. This is illustrated for the case of a simple system in Appendix B, but is true for systems with any number of degrees of freedom. The stability of the rotor-fuselage system is given by the damping characteristics of the shaft-free modes, and in the case shown in Fig.16, an analysis of the two resonance peaks of the response curves would indicate the characteristics of the rotor, with no fuselage, if allowed to translate freely in a fore-and-aft direction. The peaks of interest are associated

with minimum values of the measured impedances, and this is obvious intuitively because of the inverse relationships between impedance and response. Thus the accuracy with which the desired characteristics can be obtained depends on the accuracy with which minimum values of impedance can be measured. This emphasises the need for a high degree of accuracy in the force-measurement system. With the addition of a fuselage, the position may be rather better than that shown in Fig.16. If, in the example given, the fuselage mass is realistically represented, and the procedure is followed of adding the impedance of this mass to the rotor impedance and then inverting the sum, the resulting response curves (Fig.17) have resonance peaks close to the peaks of the original rotor impedance curves. This is so because the addition of fuselage mass reduces the free-shaft frequencies towards the fixed-shaft frequencies, and, in the limit, with a fuselage of infinite mass the two conditions will be identical. If, therefore, the fuselage impedances are large compared with the rotor impedances, the frequencies of the modes of interest in stability assessments will be fairly close to the peaks of the rotor impedances, where a high order of measurement accuracy can be obtained. In the case of ground resonance, however, the frequency of the critical fuselage support mode will be close to that of the rotor lag mode, and the fuselage impedances will be small in this frequency range. Stability assessments will then be very sensitive to measurement inaccuracies.

In passing, it may be noted that the peaks in an impedance curve are sometimes termed 'driving-point anti-resonances' of a system[2]; we have avoided this terminology because it gives less engineering 'feel' to what are, in effect, the response peaks of the system under certain conditions of restraint.

6 RESULTS

In this section, test results are given for a four-blade model rotor of semi-rigid design. The model was essentially a 1/5 scale model of the Westland Lynx main rotor designed to operate at correct Froude number. A full description of the construction is given in Ref.3, and some details are given in Appendix A of this Report.

The results presented are for zero forward speed and zero lift (Figs.18 to 25). They cover a frequency range from 1Hz to 30Hz. The results below 1Hz are inaccurate because of the very low velocities that the rig could impose on the rotor at these low frequencies. Above 30Hz problems begin to arise due to excitation of the fundamental mode of the support tower.

The characteristics of the impedances described earlier can be seen in these results. Fig.18 shows the real and imaginary parts of the pitching moment impedance due to pitch over a range of rotational speeds. At zero speed the two peaks are the blade fundamental and first overtone flap modes, and they can be seen to have quite low damping. As the rotational speed is increased, each mode is excited at two frequencies, and the variation of the actual modal frequency with rotational speed can be traced as the mean of the two frequencies at which the resonance peaks occur. It can be seen that the damping rapidly increases with rotational speed, particularly in the fundamental mode, so that at the higher speeds it is barely possible to detect either mode. In addition to these dominant modal features, there can be seen many relatively small features, some of which are due to identifiable modes of the rotor system, whilst others may arise from features of the measurement and analysis technique. In contrast, Fig.24 shows a corresponding set of fore-and-aft impedances due to fore-and-aft translation. Here one mode, the fundamental blade lag mode, dominates the picture. The damping at zero rotational speed is not high, although the presentation of all the impedance values at the same scale in Fig.24 tends to conceal this fact. As the rotational speed increases, the damping falls, and the peak impedance values increase (Fig.24 does not present a true picture in this respect because the curve plotter does not interpolate a peak between computed values). The excitation at two frequencies can just be detected at low rotational speeds, but at higher speeds, the second peak is difficult to see.

7 APPLICATION OF TEST RESULTS

Work is proceeding along several lines to use the test results to maximum advantage. So far, only applications to helicopter stability have been investigated, although the impedance approach may also provide a method of studying the forced response of a hovering helicopter.

Attempts to apply directly the method, outlined in section 5, for calculating the frequency response of the aircraft by using a computer to invert a complete matrix of impedance measurements have not been very successful. The resulting derived vector responses which should, ideally, enable the frequency and damping characteristics of all the rotor/fuselage modes to be extracted, tend to have a high degree of superimposed scatter, for the reasons that have been mentioned earlier (see section 5). It is clear that there must be some form of initial data treatment before proceeding to a stability analysis. Two approaches, that are currently under examination, are (i) reducing the number of degrees of

freedom of the rotor shaft in the preliminary analysis and (ii) smoothing the test results in the frequency range of interest. Adopting the first of these approaches in a ground resonance investigation, one might start by considering only the impedances dominated by lag-mode behaviour, and following this by including the other impedances in several stages to determine the importance of their contribution to the analysis. The second approach, of smoothing the test results, is aimed at overcoming some of the shortcomings of measurement accuracy. The risk here, of course, is that the smoothing process might remove some essential feature of the data, and it is for this reason that one needs to have a good engineering feel for the physical interpretation of the measured data. At this stage, comparisons with calculated impedances can be extremely useful, because they can guide the analyst into making correct decisions on how to 'improve' the raw data.

Another interesting possibility is that of finding analytical functions, the values of which fit the measured impedances in a specified frequency range, and then using these expressions to obtain a stability solution. The shapes of many of the impedance curves suggest that fairly simple functions could be used to obtain an accurate curve fit, and this has been found to be the case. Yet another method of analysis, suggested by Walker[4], is to obtain the modal characteristics from a vector plot of the inverse of the determinant of the impedance matrix; this has the virtue of avoiding the inversion of the matrix.

It is evident that a good deal of investigation into these and other possible methods of analysis needs to be done before a valid assessment can be made of the value of impedance measurements.

Direct comparison of measured and calculated rotor impedances has indicated that it is extremely difficult to improve an analytical model so as to eliminate or minimise differences between measured and calculated values. The difficulties arise from the large number of terms in the equations of motion and in choosing which terms to manipulate to produce a desired effect on the impedances. At the moment, therefore, impedance measurements are seen as a useful check of theory but not as a path to the improvement of theory.

8 DISCUSSION OF FUTURE WORK

A technique has been developed which can obtain, within a relatively short timescale, all the measurements on a model that are needed for an assessment of ground and air resonance instabilities, or for comparison with theory.

It remains to be seen whether the measurement accuracy is sufficiently high to overcome the inherent problems of impedance interpretation, or whether skilful handling of the measurement data can compensate for the experimental weaknesses.

Methods of improving the accuracy of the measurements will also be explored. At present the motion of the rotor shaft is measured relative to the tower by means of a velocity transducer; since the tower is also subject to vibration this is a potential source of error, particularly at the higher frequencies. This could be avoided by using accelerometers to make absolute measurements of the shaft motion and then integrating the signals to obtain velocities. Such a procedure would enable the frequency range of measurements to be extended. Although the range covered so far (up to about $2\frac{1}{2}$ times the maximum rotor speed) is sufficient for the ground and air resonance cases, which usually involve only the lower rotor modes, work on other aspects of rotor dynamics might well involve measurements at higher frequencies. This would certainly be the case for an investigation of the forced response of a helicopter.

The first use of the rig for forced response work is likely to be an investigation of the properties of rotor-mounted vibration absorbers. Since these devices are mechanical and not aerodynamic in operation, the results would apply to both the hover and forward-flight cases.

The rig itself may also be used for more general rotor dynamics work. For example it has been used as a shake test facility to determine blade mode frequency variations with rotor speed (Fig.26).

9 CONCLUSION

A technique has been developed for measuring impedances at the shaft of a rotating model helicopter rotor, using a sweep-frequency input force and digital Fourier analyser to calculate the impedances.

Measurements have been made on a dynamic model of a four blade rotor of semi-rigid design at zero lift, zero advance ratio, and over a range of rotor speeds.

The problems of interpreting and using such results are discussed in this Report, together with possible improvements and other uses for the rig.

Appendix A

ROTOR DETAILS

Rotor radius = 1.27m
Blade chord = 81mm .

Table A1

Mode frequencies (Hz)

Frequencies / Mode	Model	Scaled Lynx
1st flap	2.76	3.22
2nd flap	14.22	14.96
3rd flap	38.60	38.20
1st lag	4.40	5.01
2nd lag	40.50	41.10
1st torsion	101.0	93.0

Non-rotating mode shapes are shown in Fig.27.

Details of the rotor construction are given in Ref.3. The blades differ from the original set described in that Report, insofar as those used for the impedance measurements are true geometric replicas of the Lynx blades, incorporating both camber and twist. Minor changes in the thicknesses of the spar details were also made to improve the mass distribution of the second set of blades. The spanwise mass distribution is shown in Fig.28.

Appendix B

'SHAFT-FIXED' AND 'SHAFT-FREE' NATURAL FREQUENCIES OF A SIMPLE SYSTEM

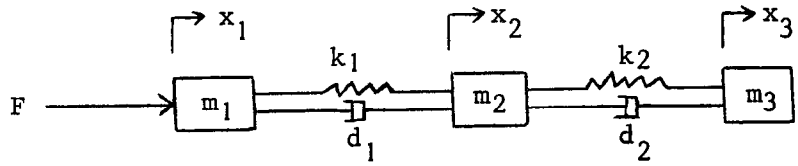

The equations of motion of the above system in which x_1 may be taken to represent 'shaft' motion, are

$$m_1\ddot{x}_1 + d_1(\dot{x}_1 - \dot{x}_2) + k_1(x_1 - x_2) = F$$

$$m_2\ddot{x}_2 + d_1(\dot{x}_2 - \dot{x}_1) + k_1(x_2 - x_1) + d_2(\dot{x}_2 - \dot{x}_3) + k_2(x_2 - x_3) = 0$$

$$m_3\ddot{x}_3 + d_2(\dot{x}_3 - \dot{x}_2) + k_2(x_3 - x_2) = 0 \ .$$

Let $F = \bar{F}e^{i\omega t}$ and assume solutions $x_1 = \bar{x}_1 e^{i\omega t}$ etc. Also, let

$$A = -\omega^2 m_1 + i\omega d_1 + k_1$$

$$B = i\omega d_1 + k_1$$

$$C = -\omega^2 m_2 + i\omega d_1 + k_1$$

$$D = i\omega d_2 + k_2$$

$$E = -\omega^2 m_3 + i\omega d_2 + k_2 \ .$$

Then

$$\begin{bmatrix} A & -B & 0 \\ -B & (C + D) & -D \\ 0 & -D & E \end{bmatrix} \begin{bmatrix} \bar{x}_1 \\ \bar{x}_2 \\ \bar{x}_3 \end{bmatrix} = \begin{bmatrix} \bar{F} \\ 0 \\ 0 \end{bmatrix}$$

therefore

$$\begin{bmatrix} \bar{x}_1 \\ \bar{x}_2 \\ \bar{x}_3 \end{bmatrix} = \frac{1}{A(E(C + D) - D^2) - B^2E} \begin{bmatrix} (E(C + D) - D^2) & BE & BD \\ BE & AE & AD \\ BD & AD & A(C + D) - B^2 \end{bmatrix} \begin{bmatrix} \bar{F} \\ 0 \\ 0 \end{bmatrix}$$

therefore $$\bar{x}_1 = \frac{E(C + D) - D^2}{A(E(C + D) - D^2) - B^2E} \bar{F} \quad .$$

An impedance is defined as

$$\frac{F}{\dot{x}} = \frac{1}{i\omega} \frac{F}{x}$$

where x and $\dot{x}$ are the amplitude and velocity of sinusoidal motion.

Therefore $$\frac{F}{\dot{x}_1} = \frac{1}{i\omega} \frac{A(E(C + D) - D^2) - B^2E}{E(C + D) - D^2} \quad .$$

The peak in this impedance will occur when $\{E(C + D) - D^2\}$ is a minimum, and it will be seen that with zero damping ($d_1 = d_2 = 0$)

$$E(C + D) - D^2 = 0$$

is the frequency equation of the system when m_1 is fixed ($x_1 = 0$).

Thus the peaks in the impedance occur at 'shaft-fixed' natural frequencies. Similarly, the inverse of the impedance,

$$\frac{\dot{x}_1}{F} = i\omega \frac{E(C + D) - D^2}{A\{E(C + D) - D^2\} - B^2E} \quad ,$$

has peaks when $A\{E(C + D) - D^2\} - B^2E$ is a minimum, and these will occur at the natural frequencies of the 'shaft-free' system.

These results can be generalised for any number of degrees of freedom.

REFERENCES

No.	Author	Title, etc.
1	R. Cansdale D.R. Gaukroger C.W. Skingle	A technique for measuring impedances of a spinning rotor. RAE Technical Report 71092 (ARC 33498) (1971)
2	F.D. Bartlett W.G. Flannelly	Application of anti-resonance theory to helicopters. 29th Annual National Forum of American Helicopter Society (1972)
3	R. Cansdale	An aeroelastic model helicopter rotor. ARC CP No.1288 (1973)
4	W.R. Walker	To assess the stability of a helicopter in air resonance from the impedances of the rotor and fuselage. Unpublished MOD(PE) Mat. (1975)

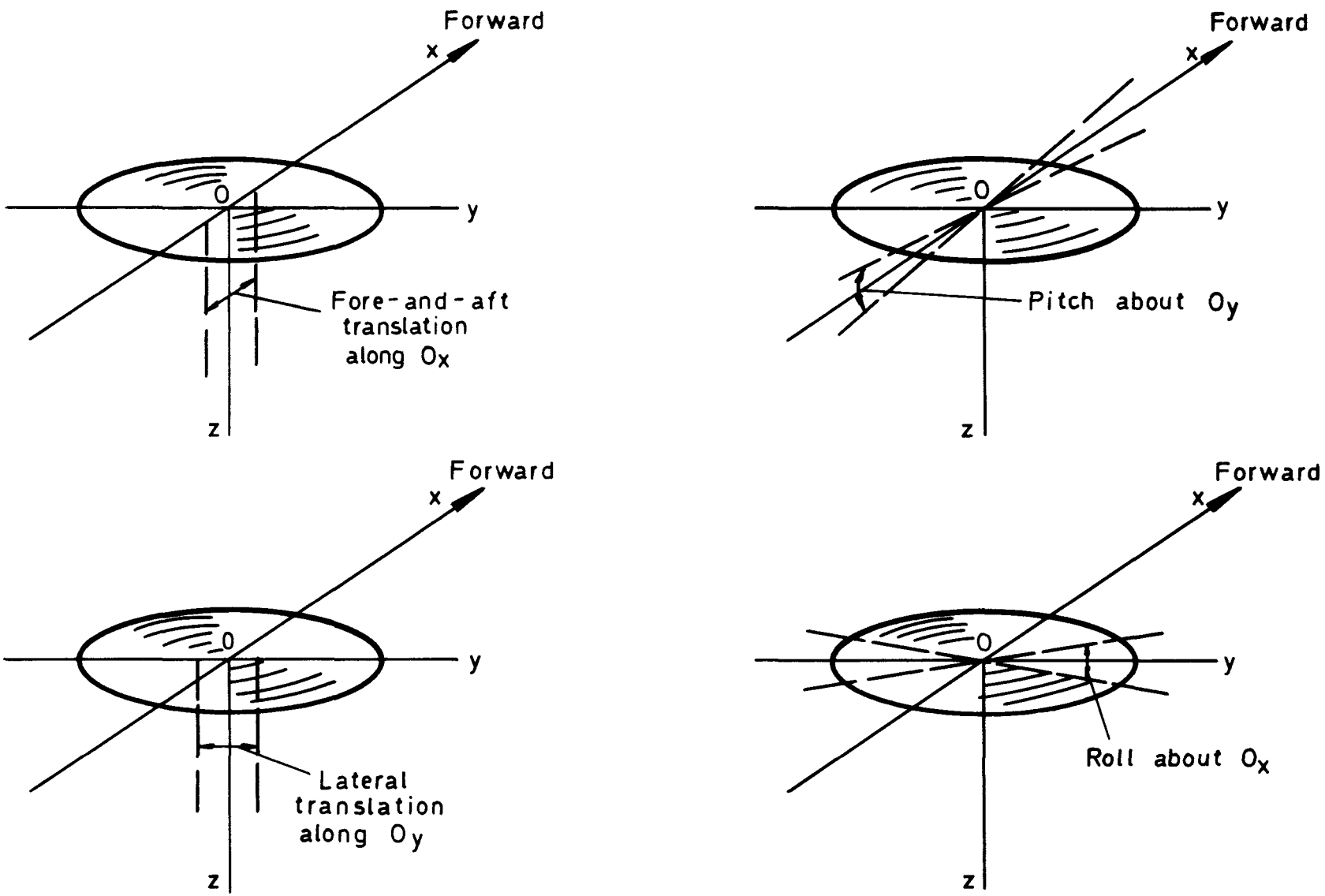

Fig.1 Rotor degrees of freedom

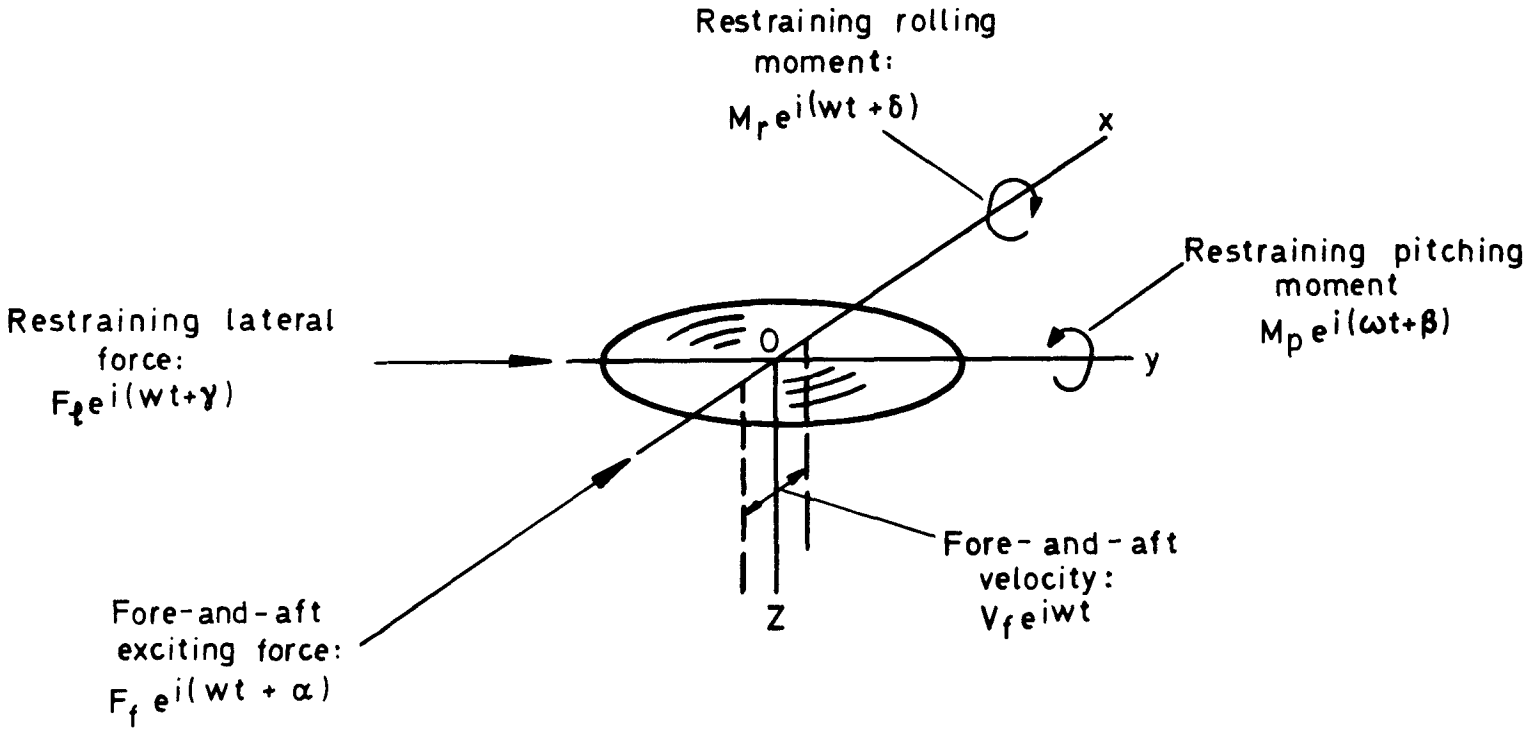

Fore-and-aft impedance $F_{xx} = \frac{F_f}{V_f} (\cos\alpha + i \sin\alpha)$

Pitch impedance $M_{\theta x} = \frac{M_p}{V_f} (\cos\beta + i \sin\beta)$

Lateral impedance $F_{yx} = \frac{F_t}{V_f} (\cos\gamma + i \sin\gamma)$

Roll impedance $M_{\phi x} = \frac{M_r}{M_f} (\cos\delta + i \sin\delta)$

Fig. 2 Impedances in fore-and-aft translation

	Froude scale	Mach scale
Linear scale ($\frac{\text{Aircraft}}{\text{Model}}$)	λ	λ
Rotational speed	$\lambda^{-\frac{1}{2}}$	λ^{-1}
Froude number	1	λ^{-1}
Mach number	$\lambda^{\frac{1}{2}}$	1
Forces — Structural	λ^3	λ^2
Forces — Centrifugal	λ^3	λ^2
Forces — Aerodynamic	λ^3	λ^2
Forces — Gravitational	λ^3	λ^3

Fig. 3 Scaling parameters

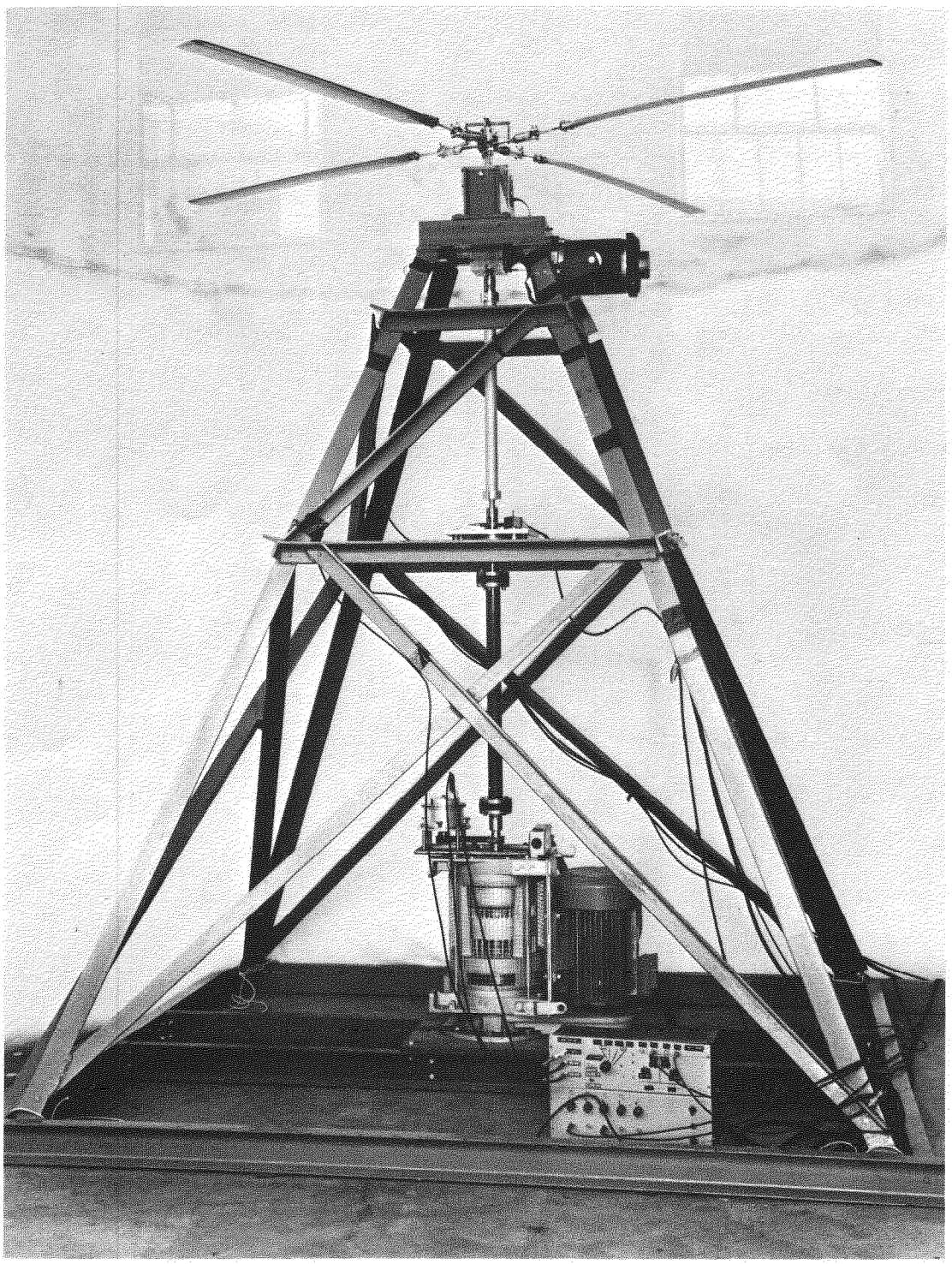

Fig.4 Rotor impedance test rig

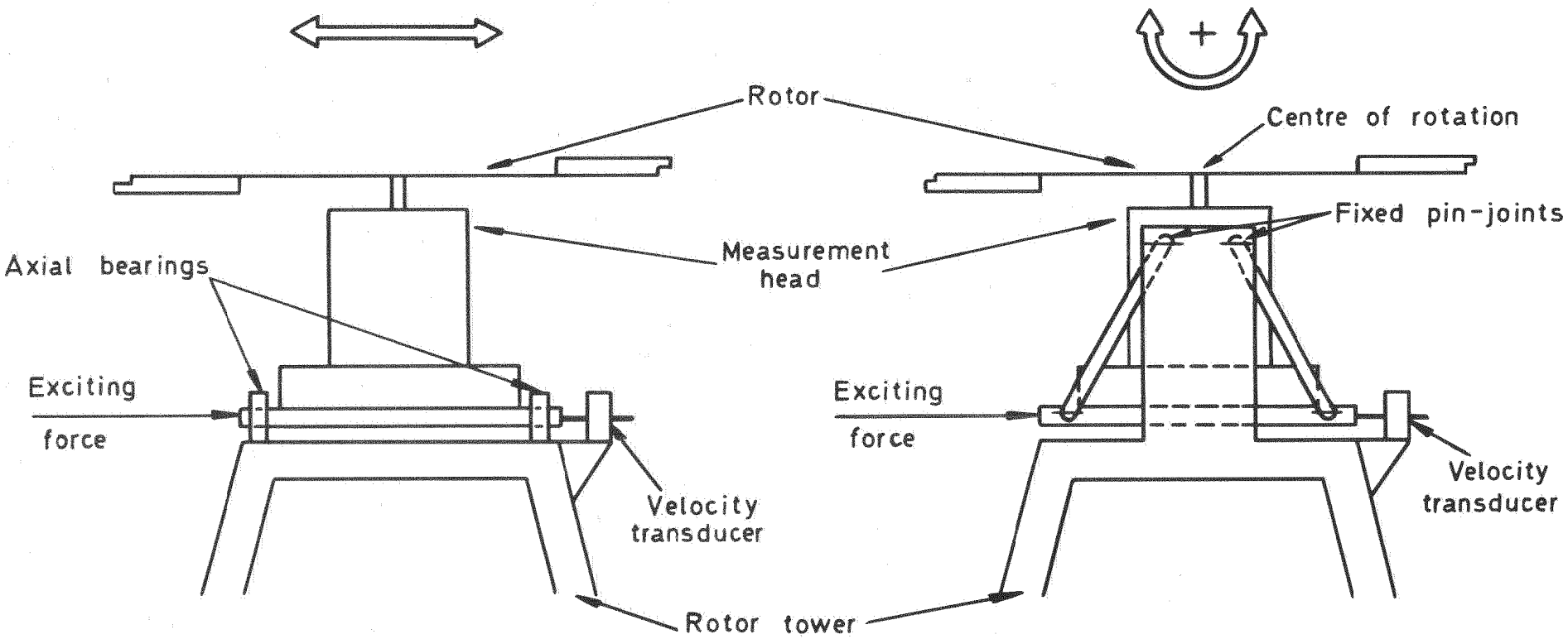

Fig. 5a & b Motion - control systems

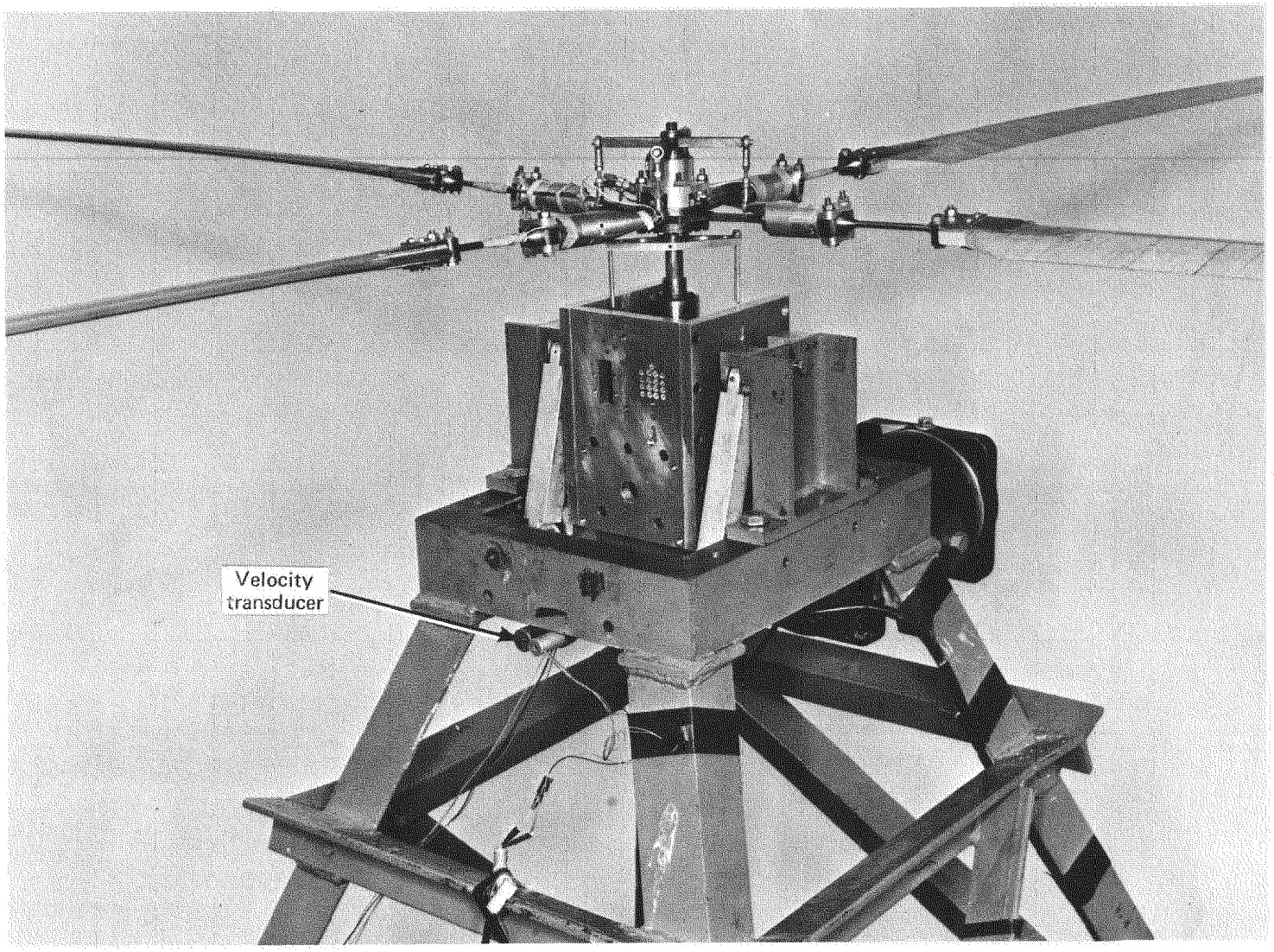

Fig.6 Rig configuration for measuring impedances due to rotor pitching

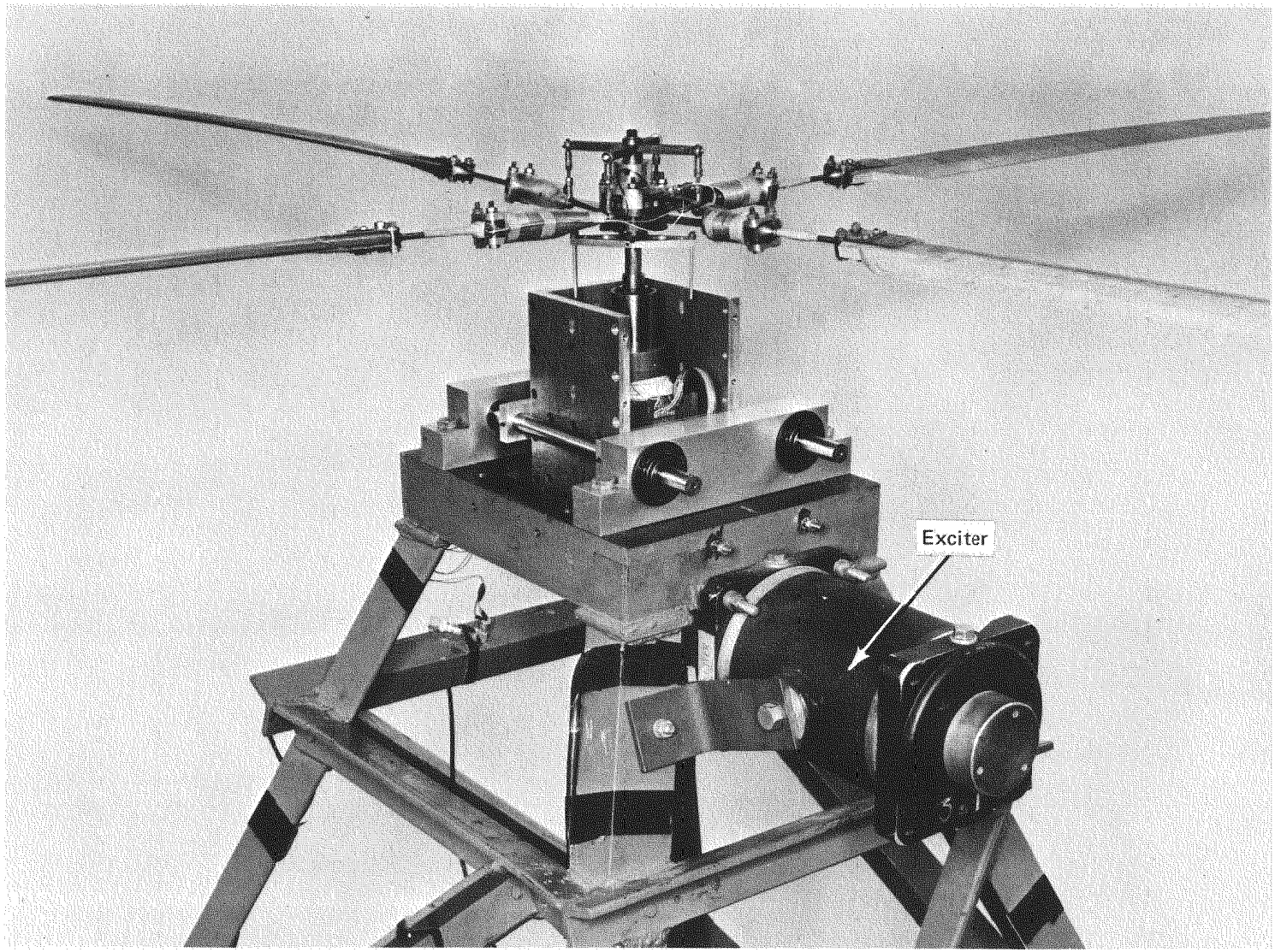

Fig.7 Rig configuration for measuring impedances due to rotor translation

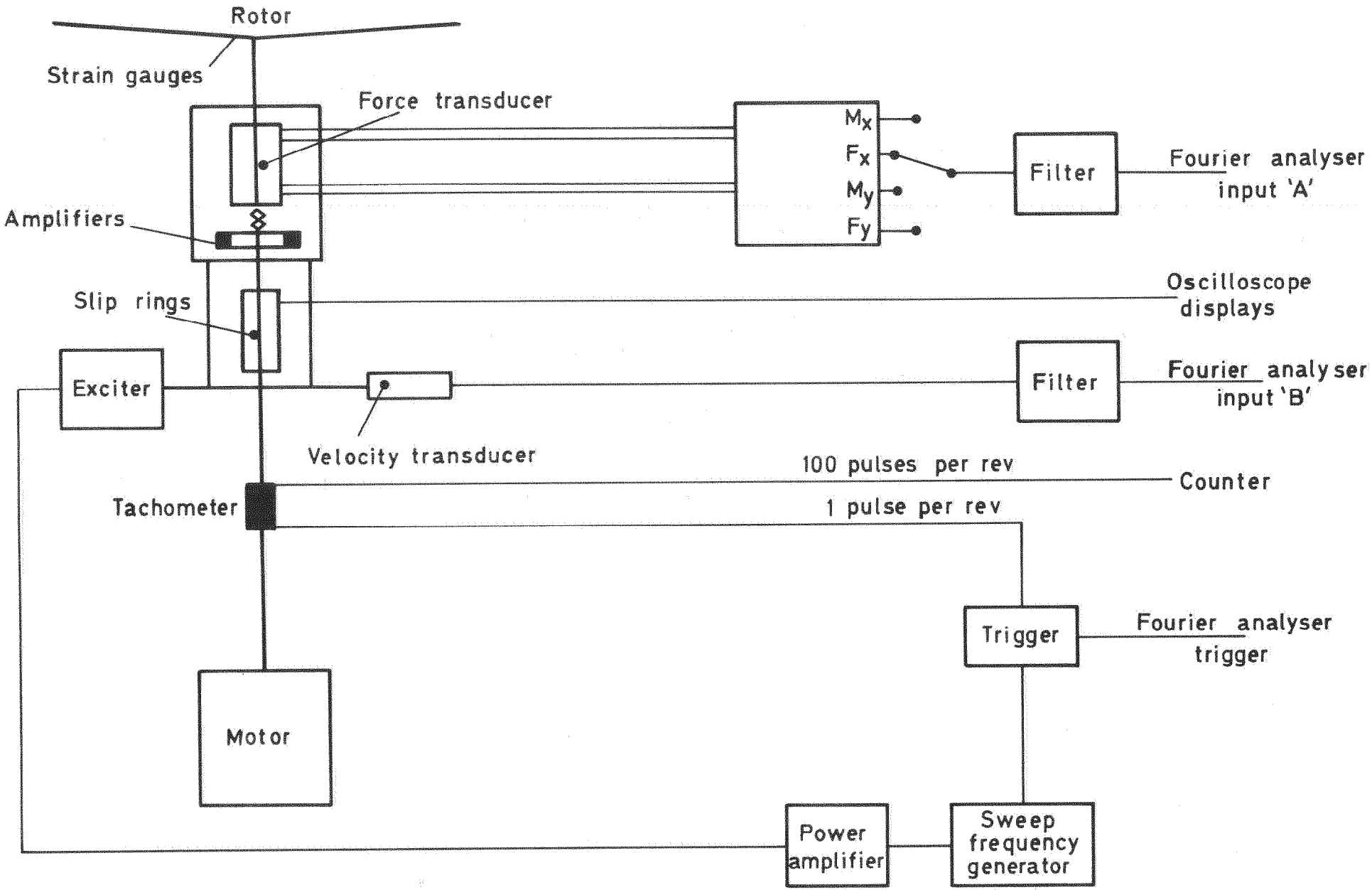

Fig. 8 Instrumentation and electrical systems

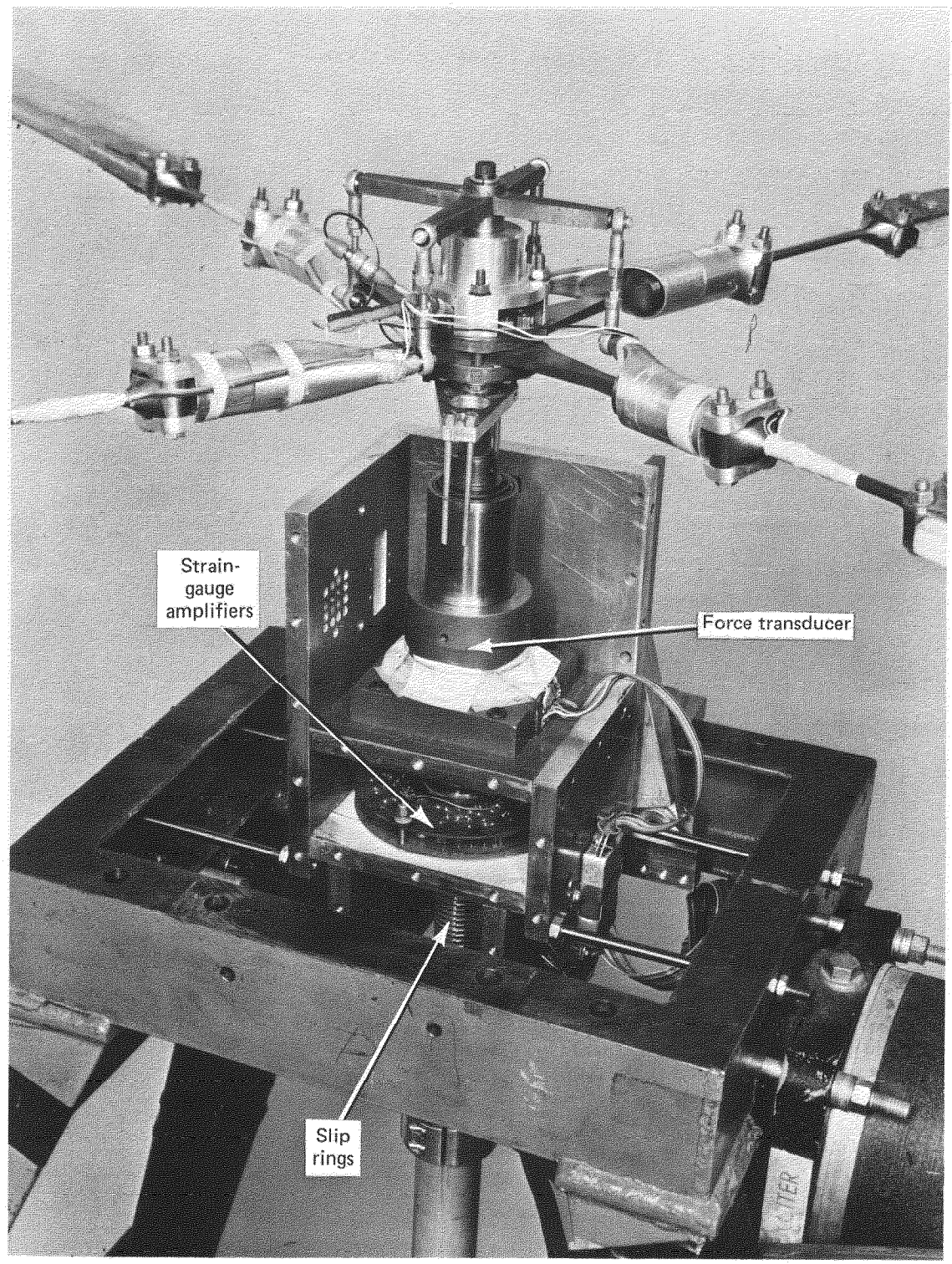

Fig.9 Internal detail of rig

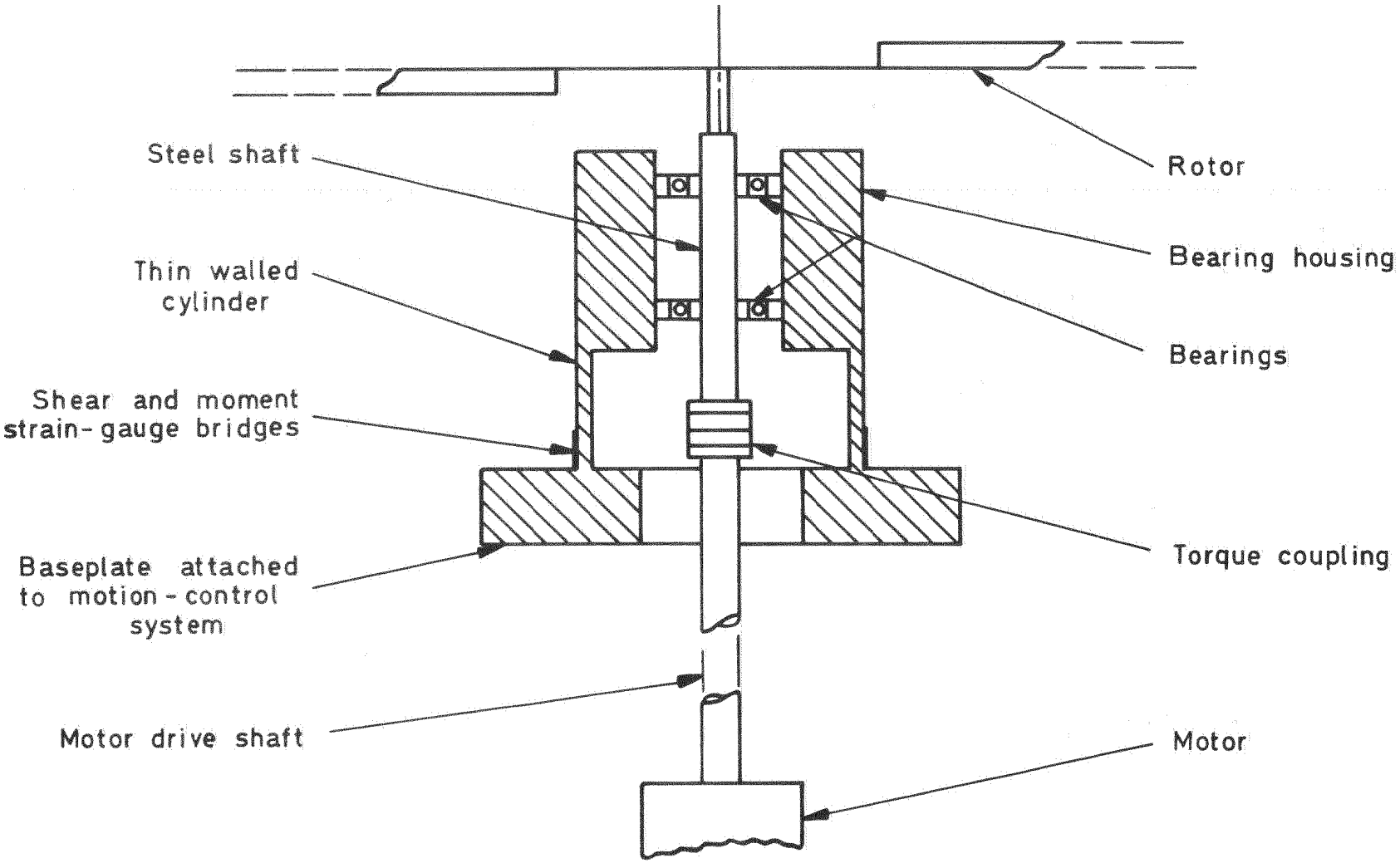

Fig.10 Measurement head

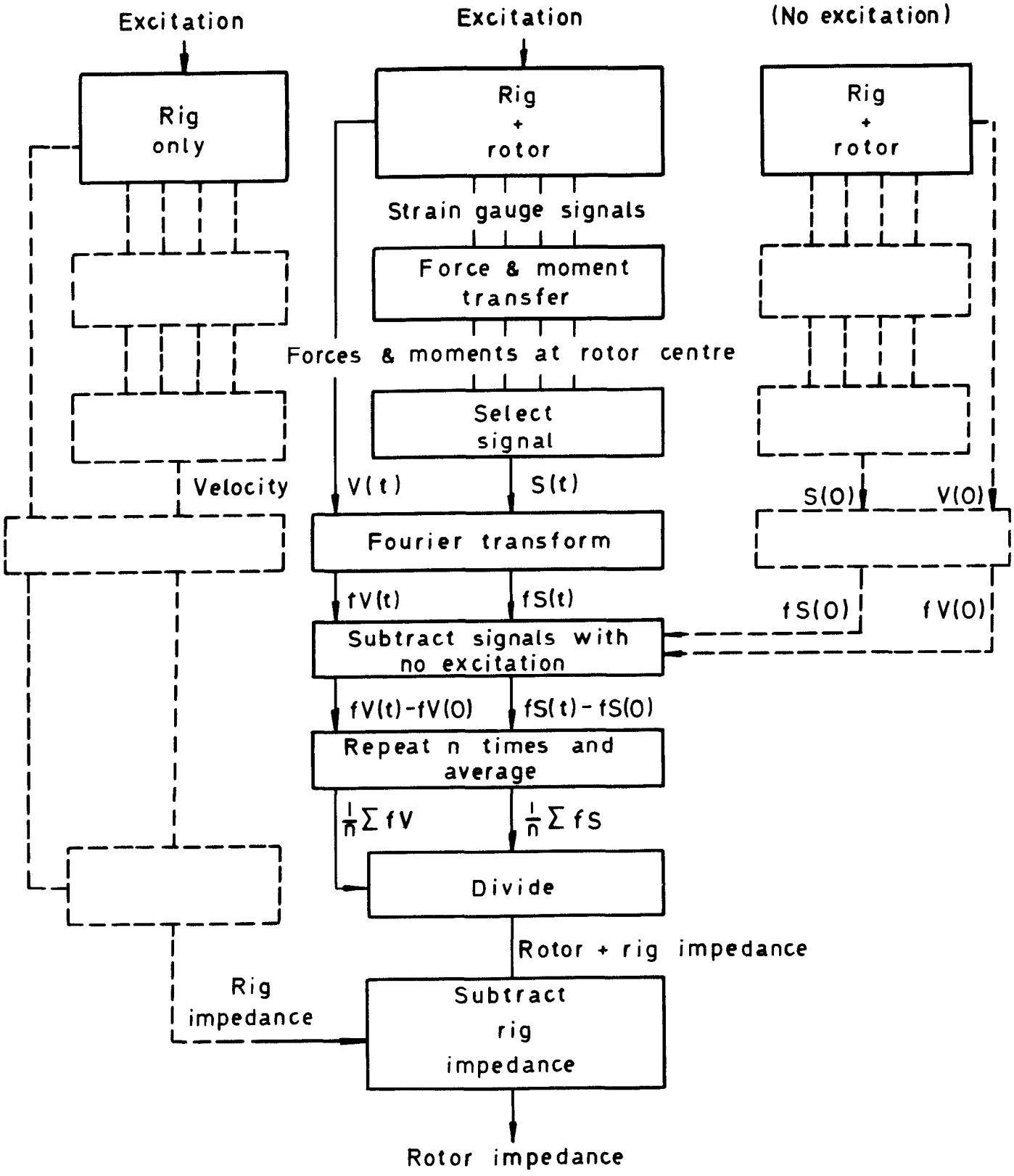

Fig.11 Analysis process

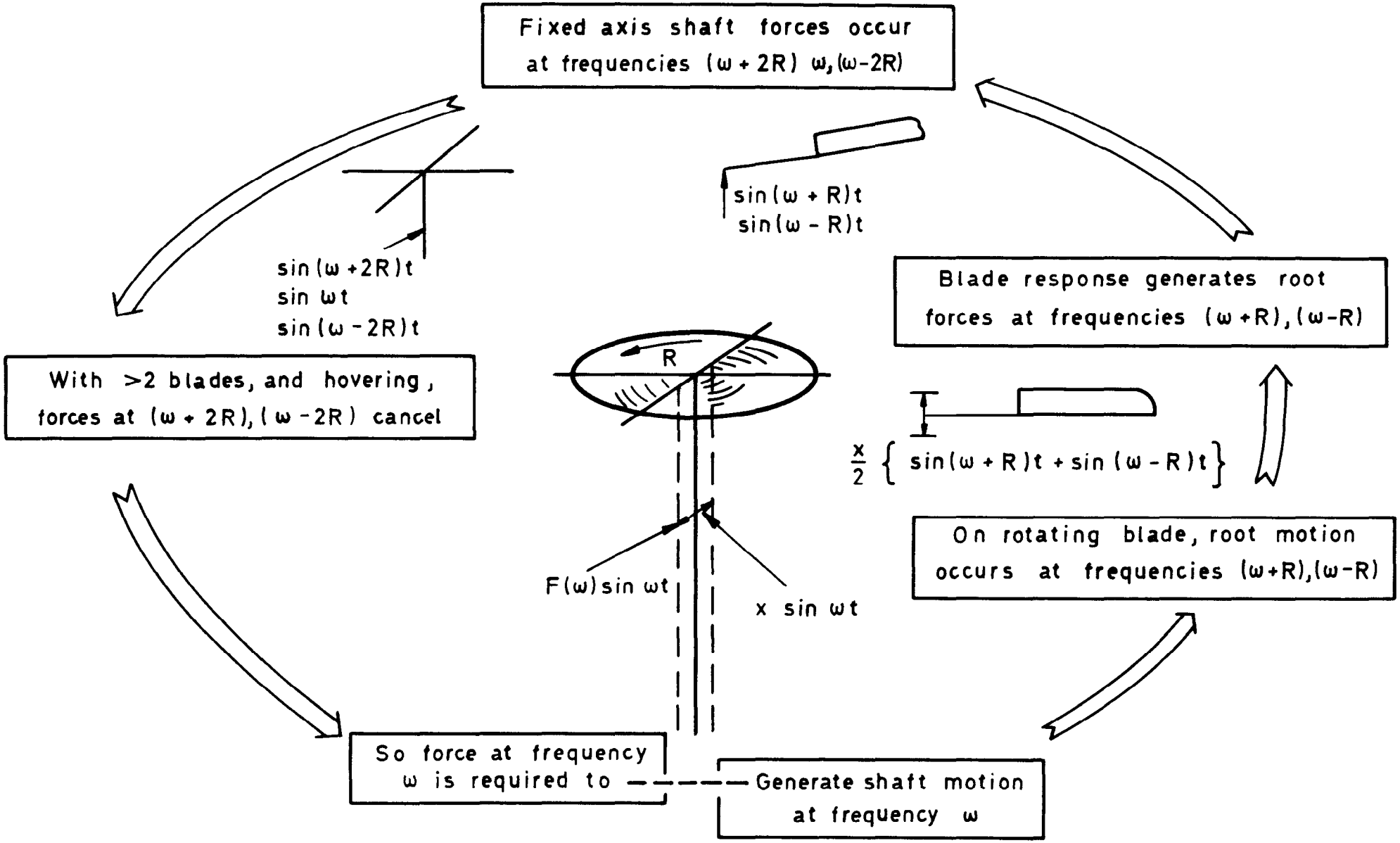

Fig.12 Excitation and response behaviour

Fore & aft translation x	Lateral translation y	Pitch θ	Roll ϕ
f_{xx}	$f_{xy}\ (=-f_{yx})$	$f_{x\theta}$	$f_{x\phi}\ (=f_{y\theta})$
f_{yx}	$f_{yy}\ (=f_{xx})$	$f_{y\theta}$	$f_{y\phi}\ (=-f_{x\theta})$
$m_{\theta x}$	$m_{\theta y}\ (=m_{\phi x})$	$m_{\theta\theta}$	$m_{\theta\phi}\ (=-m_{\phi\theta})$
$m_{\phi x}$	$m_{\phi x}\ (=-m_{\theta x})$	$m_{\phi\theta}$	$m_{\phi\phi}\ (=m_{\theta\theta})$

Measured — Measured

Fig.13 Matrix of rotor impedances in hover

M = Mass of fuselage

$M\bar{z}$ = Mass moment of fuselage about rotor

Mp^2, Mr^2 = Mass MI of fuselage in pitch & roll about rotor

$\frac{Mg\bar{z}}{\omega^2}$ = Gravitational component of MI about rotor

$i\omega M$	0	$i\omega M\bar{z}$	0
0	$i\omega M$	0	$i\omega M\bar{z}$
$i\omega M\bar{z}$	0	$i\omega\left(Mp^2 - \frac{Mg\bar{z}}{\omega^2}\right)$	0
0	$i\omega M\bar{z}$	0	$i\omega\left(Mr^2 - \frac{Mg\bar{z}}{\omega^2}\right)$

Assumptions : (i) Rigid fuselage

(ii) Fuselage cg vertically below rotor centre

Fig.14 Matrix of fuselage impedances in hover

Rotor impedances

$$\begin{bmatrix} f_{xx} & f_{xy} & f_{x\theta} & f_{x\phi} \\ f_{yx} & f_{yy} & f_{y\theta} & f_{y\phi} \\ m_{\theta x} & m_{\theta y} & m_{\theta\theta} & m_{\theta\phi} \\ m_{\phi x} & m_{\phi y} & m_{\phi\theta} & m_{\phi\phi} \end{bmatrix} + i\omega M \begin{bmatrix} 1 & 0 & \bar{z} & 0 \\ 0 & 1 & 0 & \bar{z} \\ \bar{z} & 0 & \left(p^2 - \frac{g\bar{z}}{\omega^2}\right) & 0 \\ 0 & \bar{z} & 0 & \left(r^2 - \frac{g\bar{z}}{\omega^2}\right) \end{bmatrix} = [\Phi]$$

Fuselage impedances

Equations of motion of rotor + fuselage:-

a Free oscillations

$$[\Phi]\begin{bmatrix} x \\ y \\ \theta \\ \phi \end{bmatrix} = \begin{bmatrix} 0 \\ 0 \\ 0 \\ 0 \end{bmatrix}$$

b Forced oscillations

$$[\Phi]\begin{bmatrix} x \\ y \\ \theta \\ \phi \end{bmatrix} = \begin{bmatrix} F_1 \\ F_2 \\ F_3 \\ F_4 \end{bmatrix}$$

Modal frequencies and damping ratios given by:-

a Roots of:
$\det[\Phi] = 0$

b Analysis of response vector:

$$V_\alpha = [\alpha_1\ \alpha_2\ \alpha_3\ \alpha_4][\Phi]^{-1}\begin{bmatrix} F_1 \\ F_2 \\ F_3 \\ F_4 \end{bmatrix}$$

Fig.15 Analysis of impedance data

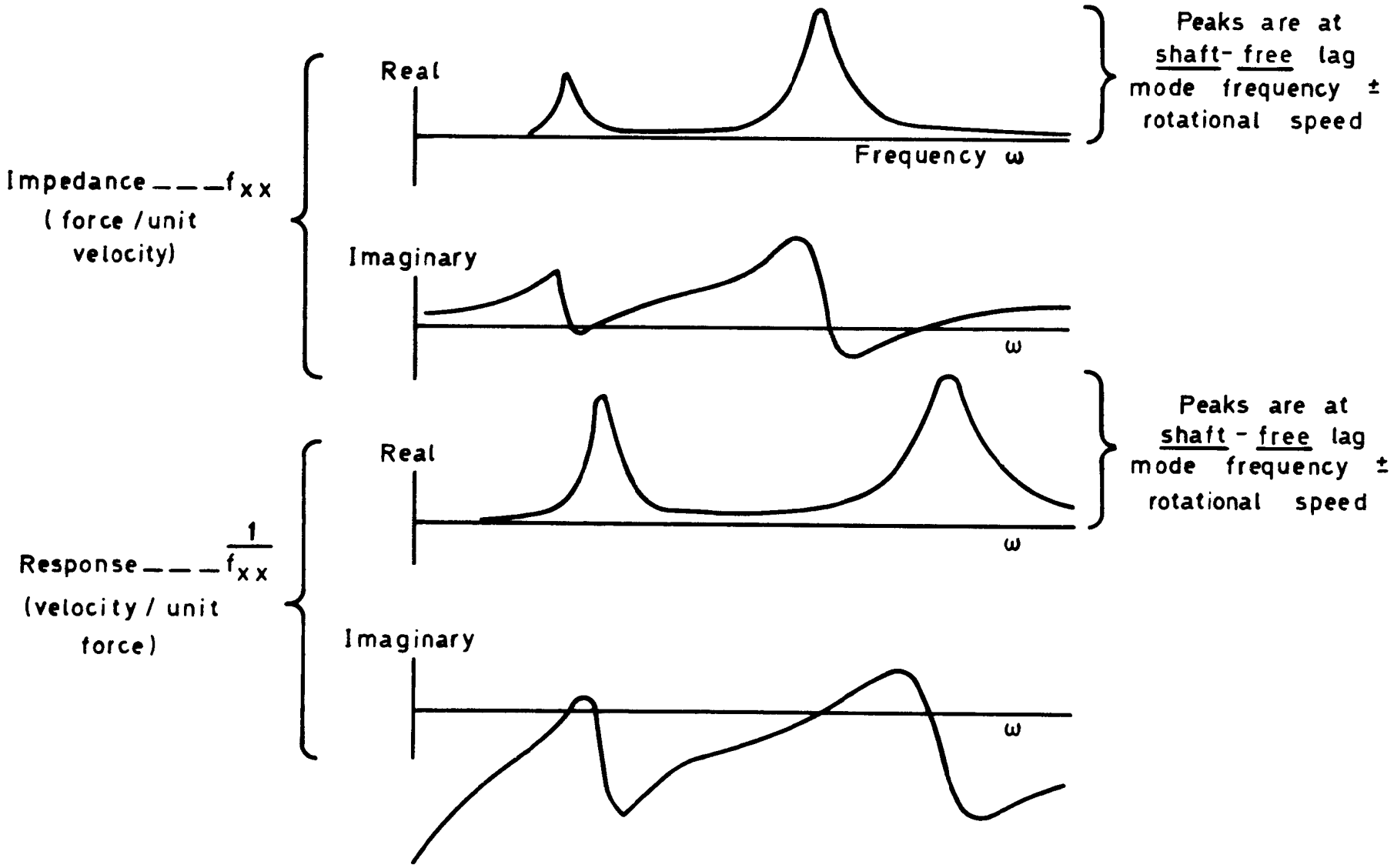

Fig. 16 Example of impedance inversion

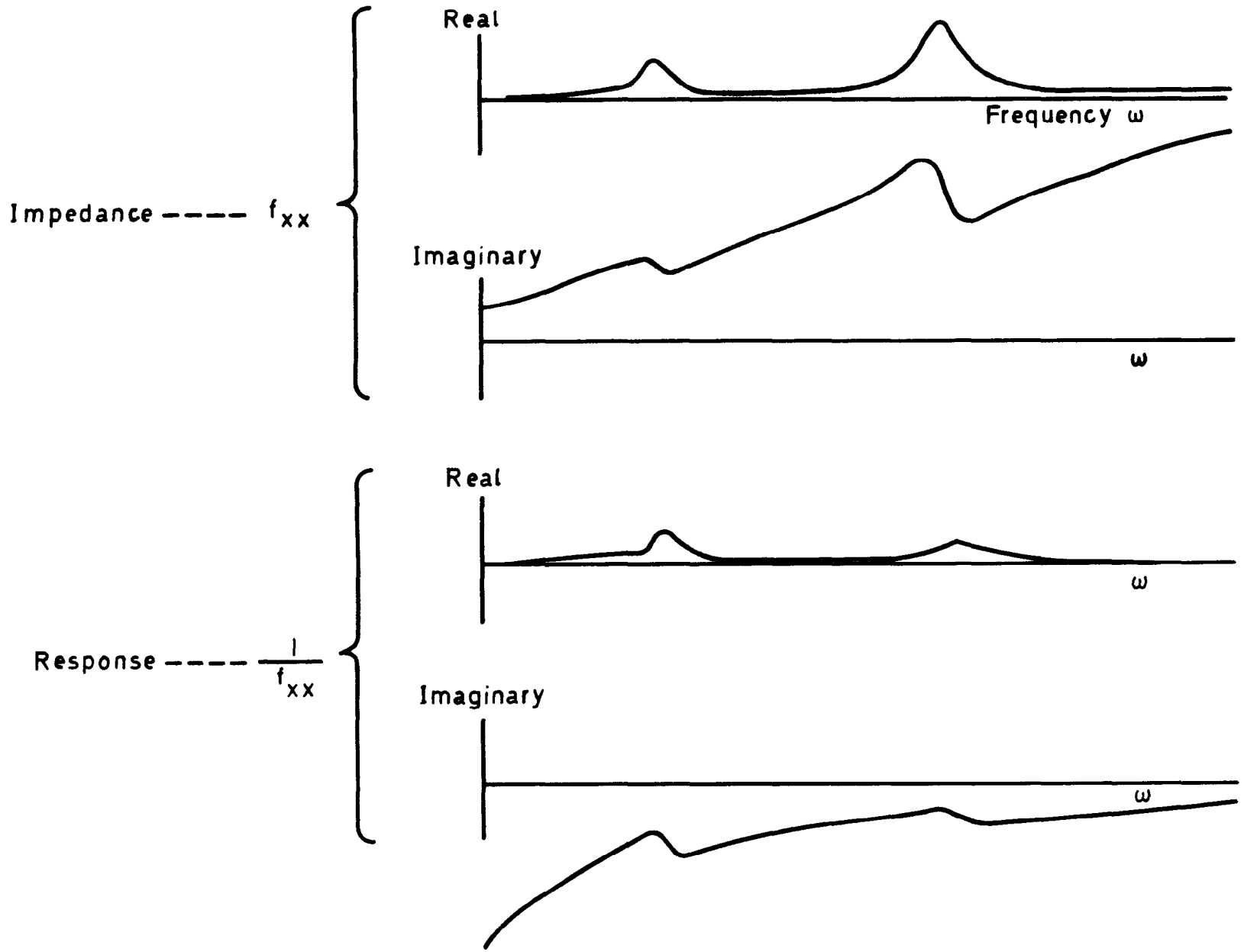

Fig. 17 Impedance and response of rotor + fuselage

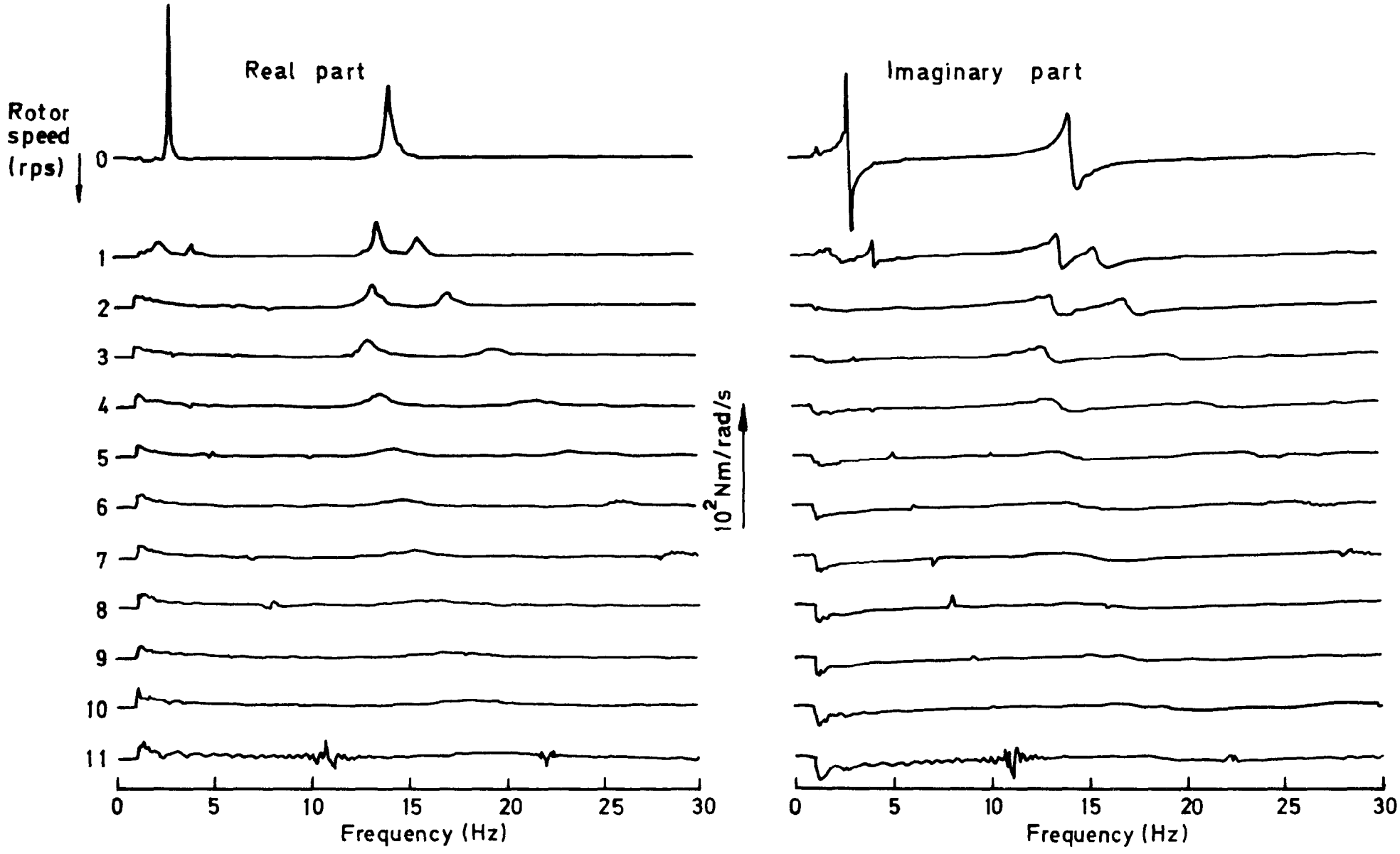

Fig.18 $m_{\theta\theta}$: pitching impedance due to pitch

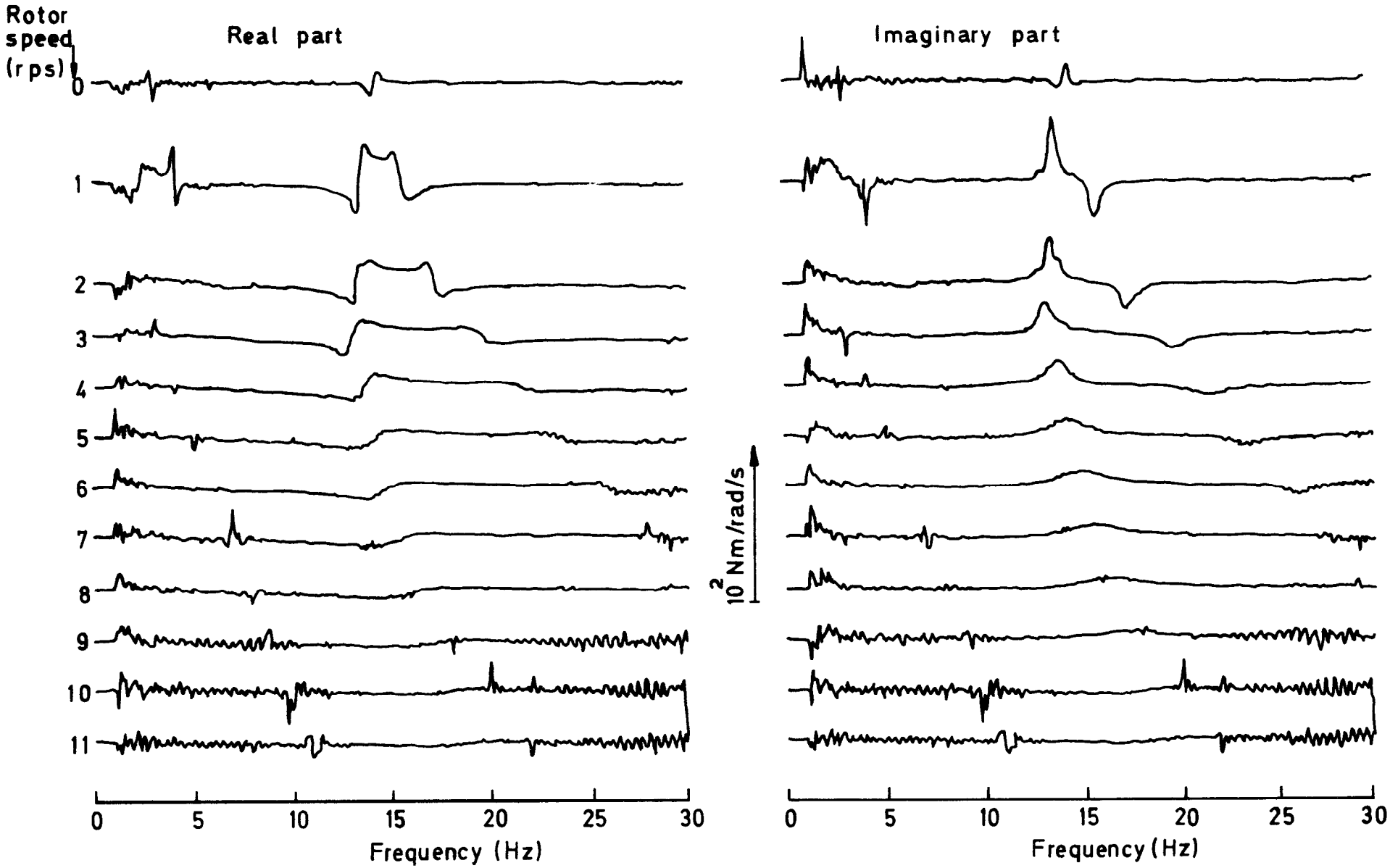

Fig. 19 $m_{\phi\theta}$: rolling impedance due to pitch

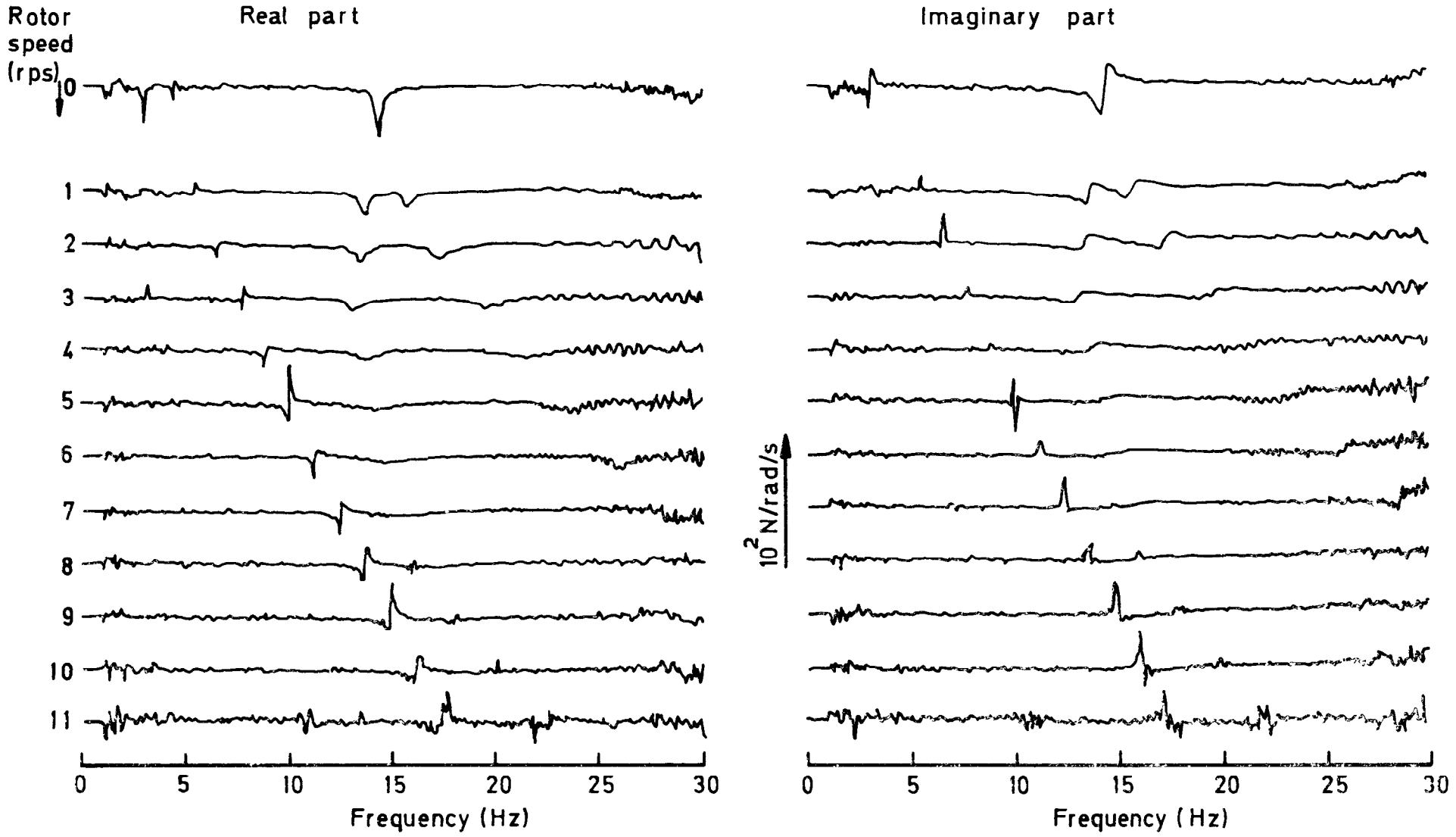

Fig 20 $f_{x\theta}$: fore-and-aft impedance due to pitch

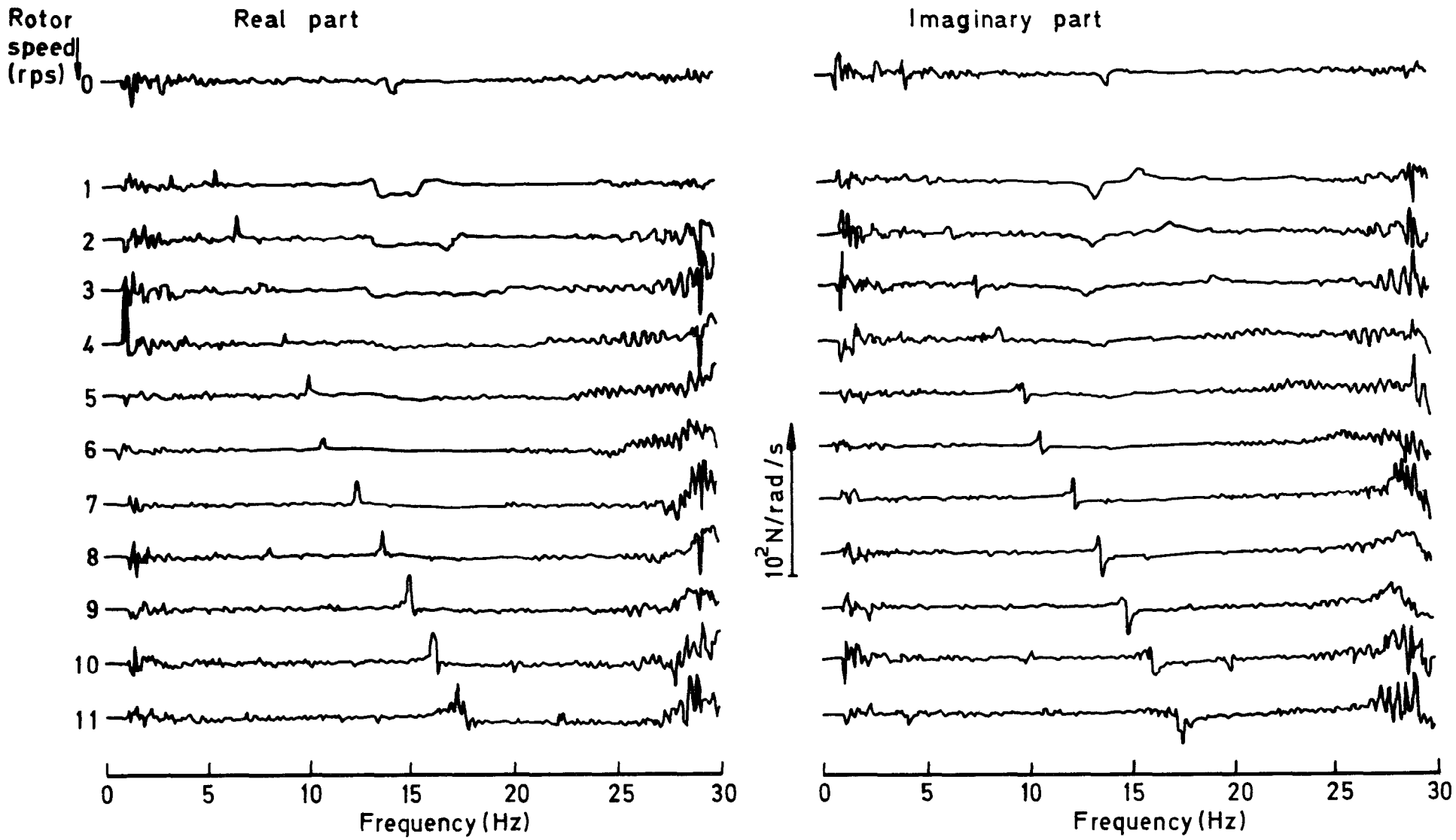

Fig.21 $f_{y\theta}$: lateral impedance due to pitch

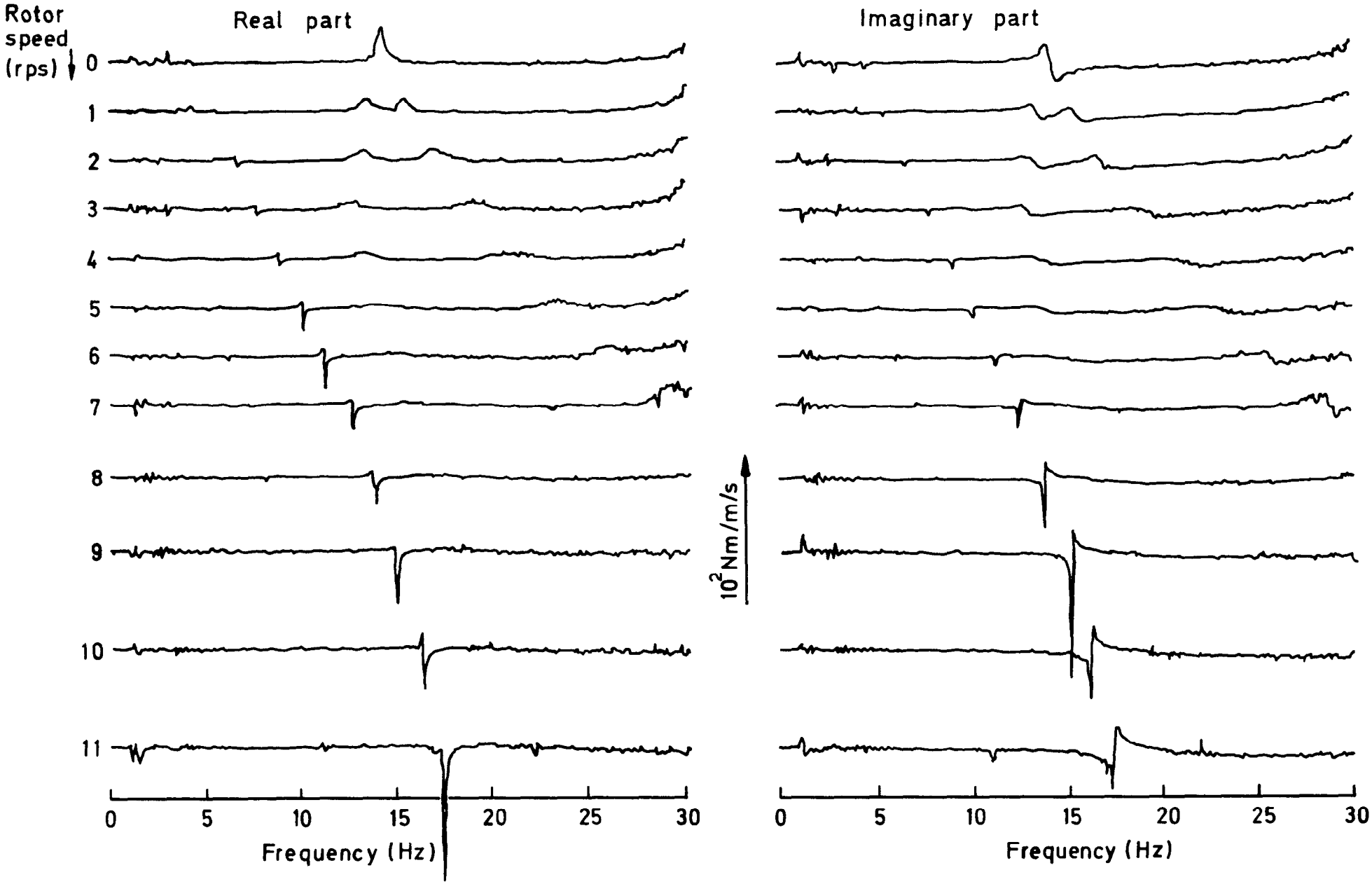

Fig.22 $m_{\theta x}$: pitching impedance due to fore-and-aft translation

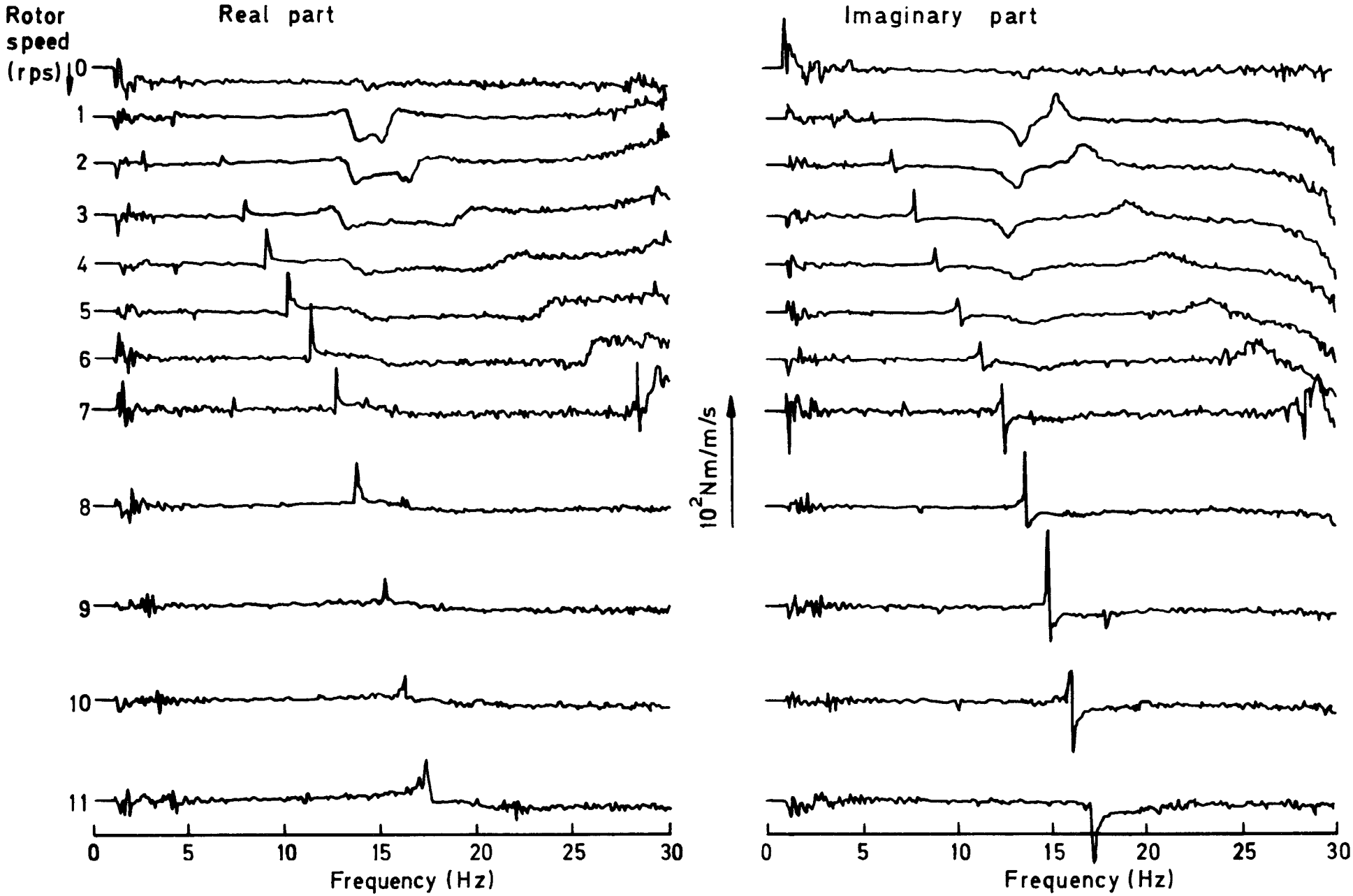

Fig 23 $m_{\phi x}$: rolling impedance due to fore-and-aft translation

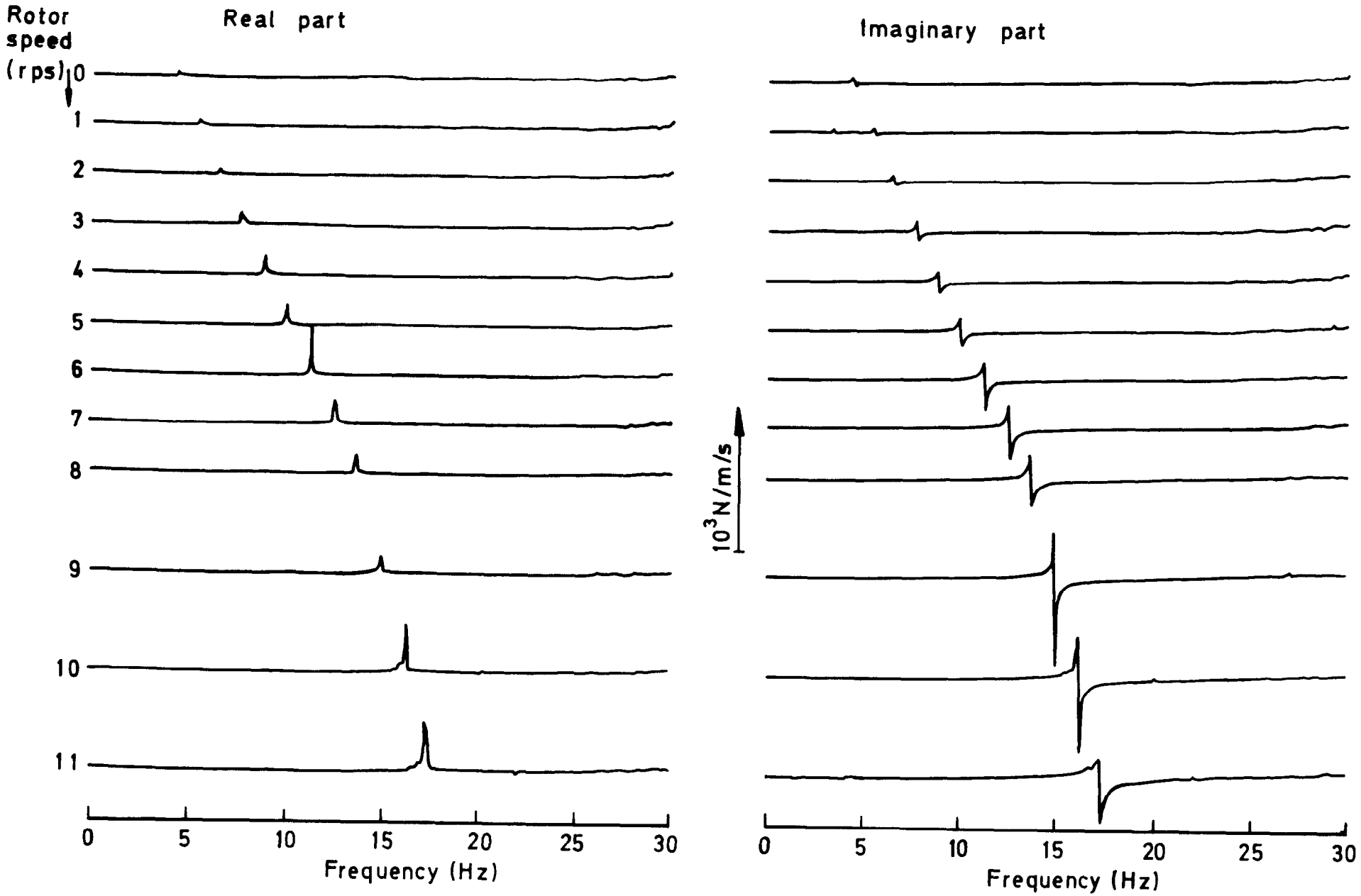

Fig.24 f_{xx} : fore-and-aft impedance due to fore-and-aft translation

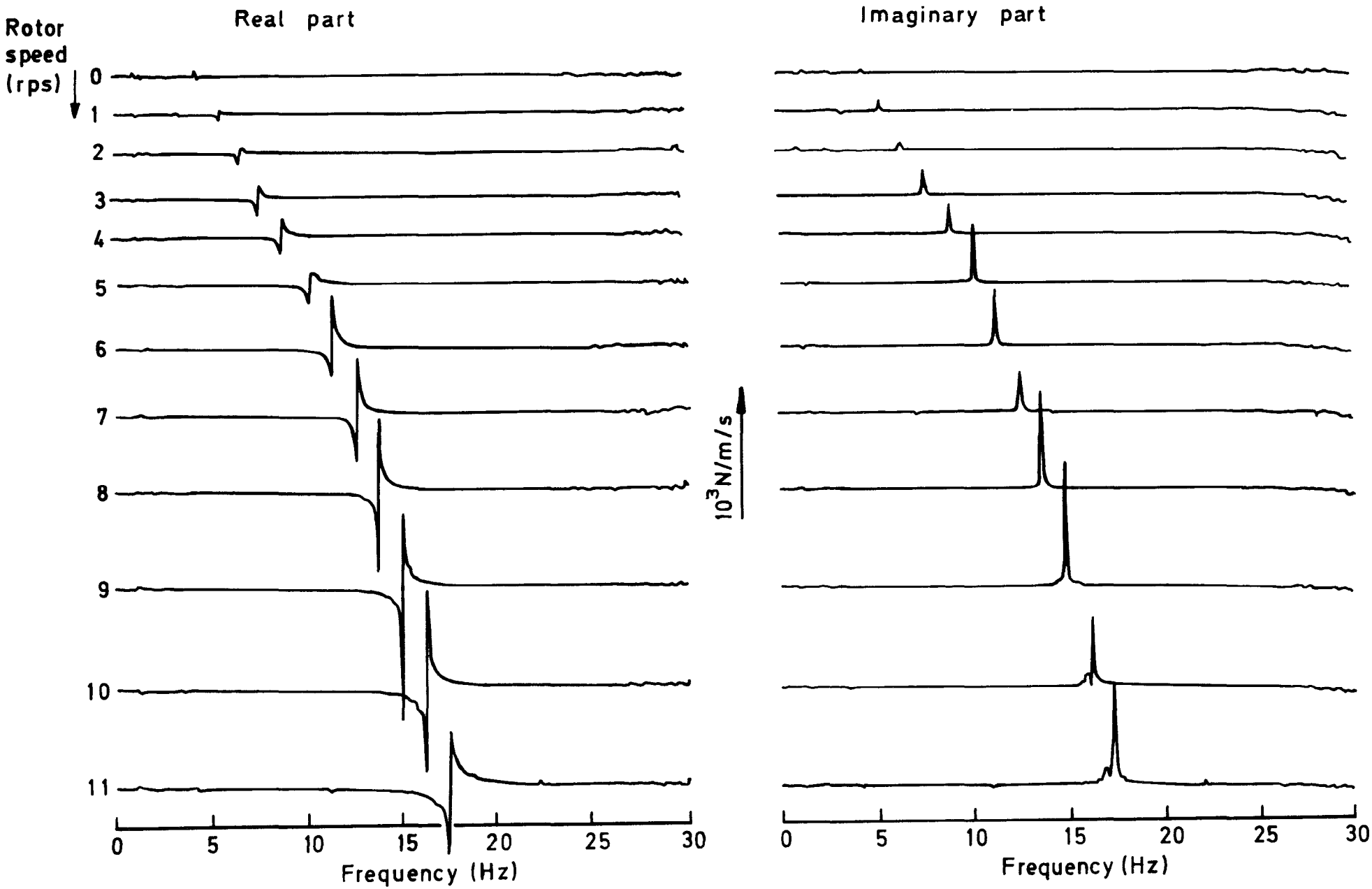

Fig.25 f_{yx} : lateral impedance due to fore-and-aft translation

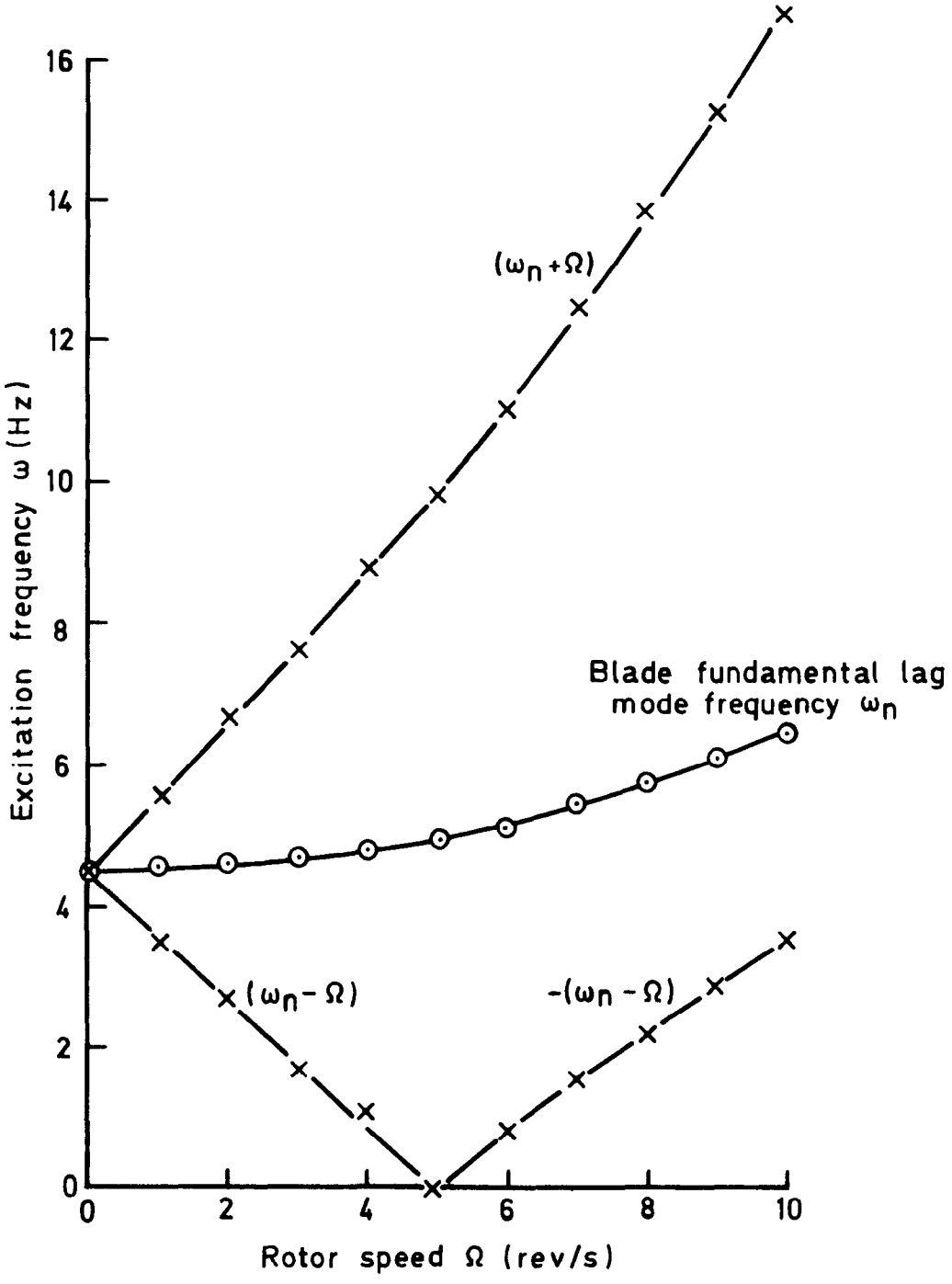

Fig.26 Variation of lag mode frequency

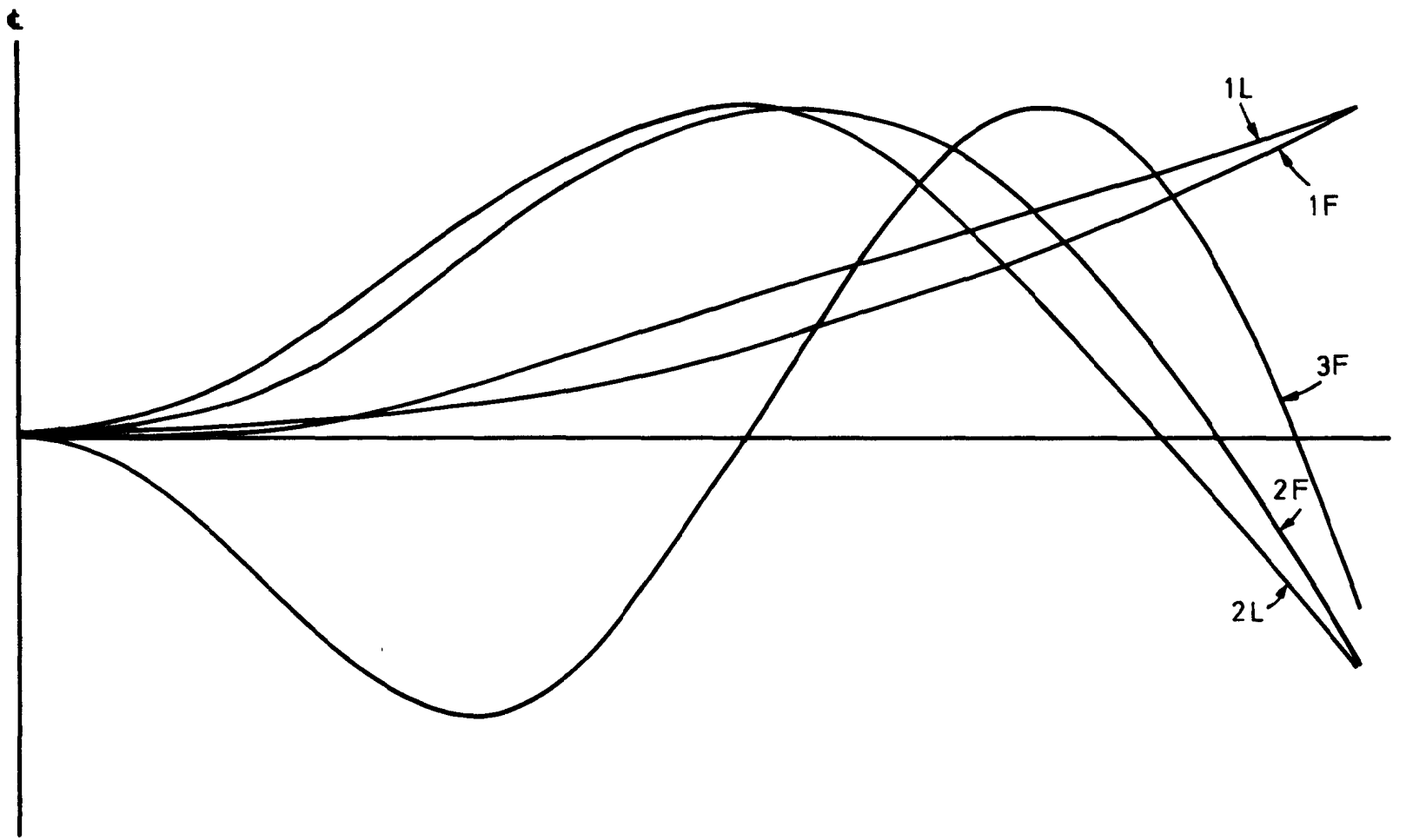

Fig.27 Non-rotating mode shapes

Printed in England for Her Majesty's Stationery Office by the Royal Aircraft Establishment, Farnborough Dd 587483 K5 11/78

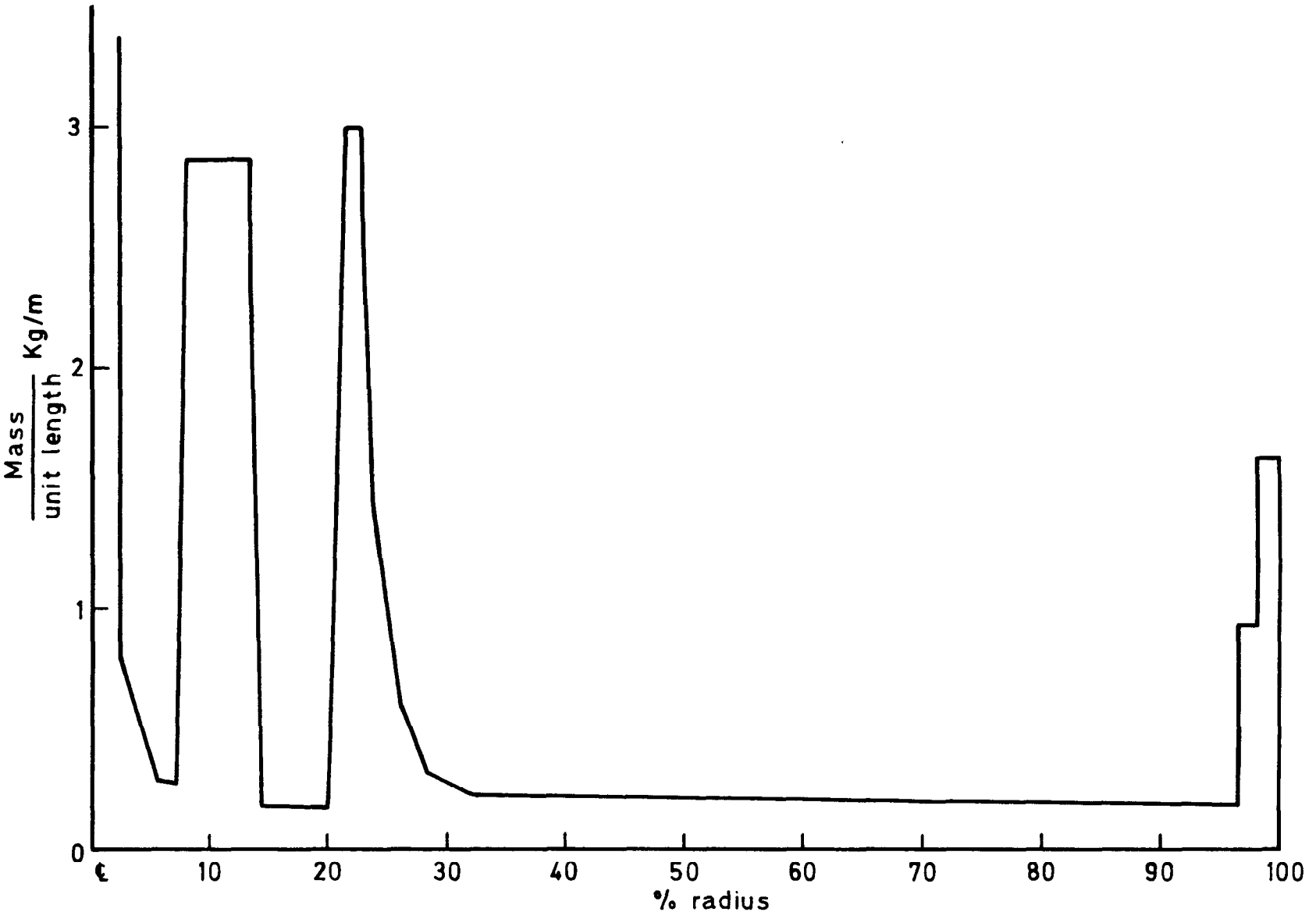

Fig.28 Blade mass distribution

ARC CP No.1389
July 1976

534.231.3 :
533.662.6 :
533.661

R. Cansdale
D.R. Gaukroger

IMPEDANCE MEASUREMENTS ON A SPINNING MODEL HELICOPTER ROTOR

The technique for measuring rotor impedances at the shaft of a model rotor has been further developed. The present technique is described in the Report, and values of impedance are presented for a four-blade rotor of semi-rigid design operating at zero lift, zero advance ratio, and a range of rotational speeds. The problems of interpreting and applying rotor impedances are discussed.

ARC CP No.1389
July 1976

534.231.3 :
533.662.6 :
533.661

R. Cansdale
D.R. Gaukroger

IMPEDANCE MEASUREMENTS ON A SPINNING MODEL HELICOPTER ROTOR

The technique for measuring rotor impedances at the shaft of a model rotor has been further developed. The present technique is described in the Report, and values of impedance are presented for a four-blade rotor of semi-rigid design operating at zero lift, zero advance ratio, and a range of rotational speeds. The problems of interpreting and applying rotor impedances are discussed.

Cut here

ARC CP No.1389
July 1976

534.231.3 :
533.662.6 :
533.661

R. Cansdale
D.R. Gaukroger

IMPEDANCE MEASUREMENTS ON A SPINNING MODEL HELICOPTER ROTOR

The technique for measuring rotor impedances at the shaft of a model rotor has been further developed. The present technique is described in the Report, and values of impedance are presented for a four-blade rotor of semi-rigid design operating at zero lift, zero advance ratio, and a range of rotational speeds. The problems of interpreting and applying rotor impedances are discussed.

Cut here

ARC CP No.1389
July 1976

534.231.3 :
533.662.6 :
533.661

R. Cansdale
D.R. Gaukroger

IMPEDANCE MEASUREMENTS ON A SPINNING MODEL HELICOPTER ROTOR

The technique for measuring rotor impedances at the shaft of a model rotor has been further developed. The present technique is described in the Report, and values of impedance are presented for a four-blade rotor of semi-rigid design operating at zero lift, zero advance ratio, and a range of rotational speeds. The problems of interpreting and applying rotor impedances are discussed.

DETACHABLE ABSTRACT CARDS

DETACHABLE ABSTRACT CARDS

1978

Published by
HER MAJESTY'S STATIONERY OFFICE

Government Bookshops
49 High Holborn, London WC1V 6HB
13a Castle Street, Edinburgh EH2 3AR
41 The Hayes, Cardiff CF1 1JW
Brazennose Street, Manchester M60 8AS
Southey House, Wine Street, Bristol BS1 2BQ
258 Broad Street, Birmingham B1 2HE
80 Chichester Street, Belfast BT1 4JY

Government Publications are also available through booksellers

C.P. No. 1389

ISBN 011 471135 6